



# Scenarios of Deoxygenation of the Eastern Tropical North Pacific During the Past Millennium as a Window Into the Future of Oxygen Minimum Zones

Konstantin Choumiline<sup>1\*</sup>, Ligia Pérez-Cruz<sup>2</sup>, Andrew B. Gray<sup>3</sup>, Steven M. Bates<sup>1</sup> and Timothy W. Lyons<sup>1</sup>

<sup>1</sup> Department of Earth and Planetary Sciences, University of California, Riverside, Riverside, CA, United States, <sup>2</sup> Instituto de Geofísica, Universidad Nacional Autónoma de México, Mexico City, Mexico, <sup>3</sup> Department of Environmental Sciences, University of California, Riverside, Riverside, CA, United States

## OPEN ACCESS

### Edited by:

Babette Hoogakker,  
Heriot-Watt University,  
United Kingdom

### Reviewed by:

Nicolas Tribouillard,  
Lille University of Science and  
Technology, France  
Laetitia Pichevin,  
University of Edinburgh,  
United Kingdom

### \*Correspondence:

Konstantin Choumiline  
konstantin.choumiline@email.ucr.edu

### Specialty section:

This article was submitted to  
Marine Biogeochemistry,  
a section of the journal  
Frontiers in Earth Science

**Received:** 20 September 2018

**Accepted:** 28 August 2019

**Published:** 26 September 2019

### Citation:

Choumiline K, Pérez-Cruz L, Gray AB,  
Bates SM and Lyons TW (2019)  
Scenarios of Deoxygenation of the  
Eastern Tropical North Pacific During  
the Past Millennium as a Window Into  
the Future of Oxygen Minimum Zones.  
*Front. Earth Sci.* 7:237.  
doi: 10.3389/feart.2019.00237

Diverse studies predict global expansion of Oxygen Minimum Zones (OMZs) as a consequence of anthropogenic global warming. While the observed dissolved oxygen concentrations in many coastal regions are slowly decreasing, sediment core paleorecords often show contradictory trends. This is the case for numerous high-resolution reconstructions of oxygenation in the Eastern Tropical North Pacific (ETNP). While major shifts in redox conditions of the ETNP are dominated by glacial-interglacial cycling, important fluctuations also occur in response to minor climatic and oceanographic perturbations. It is important to understand these scenarios of past redox variation, as they are the closest analog for near future climate and oceanographic change. We present recently collected sediment core proxy records from the Gulf of California in which we reproduce the variability of productivity and oxygenation of the ETNP OMZ during the past millennium. We emphasize paleoproductivity ( $C_{org}$ , Ni,  $Ba_{excess}$ ) and paleoredox indicators (Mo, Cd, V,  $U_{auth}$ ) in sediment cores collected in Alfonso and La Paz basins and compare these OMZ records with other archives of the Eastern Pacific. Our findings indicate that the OMZ expanded in response to increased upwelling and productivity during cold intervals of the early 1400s, early 1500s, late 1600s, and early 1800s AD (evidenced by higher Ni, V, Cd, Mo, and  $U_{auth}$ ). The most hypoxic times corresponded to the beginning of the Little Ice Age (expressed in elevated Mo). Significant OMZ contractions occurred around late 1300s, early 1700s, and late 1900s AD after reoxygenation events that were instigated by low productivity (lower Ni, V, Cd, Mo, and  $U_{auth}$ ). The mechanisms that control decadal-to-centennial oxygen variability in the ETNP remain unidentified but are likely influenced by solar forcing not only driving migrations of the Intertropical Convergence Zone (ITCZ) but more importantly changes in the intensity of the Pacific Walker Circulation (PWC). During the Little Ice Age solar irradiance was at its lowest for the past millennium, which strengthened the PWC. This pattern contributed to more frequent La Niña-like conditions, which enhanced upwelling of nutrient-rich waters in the west coast of North America, driving productivity and reducing bottom oxygen levels, as seen in our ETNP records.

**Keywords:** Oxygen Minimum Zones (OMZs), Eastern Tropical North Pacific (ETNP), primary productivity, deoxygenation, hypoxia, paleoredox, redox-sensitive trace elements, authigenic uranium

## INTRODUCTION

Numerous experimental, observational, and numerical model studies predict global expansion of Oxygen Minimum Zones (OMZ) linked to human induced climate change (Keeling et al., 2010; Gilly et al., 2013; Howes et al., 2015; Praetorius et al., 2015; Levin, 2018). The Eastern Tropical North Pacific (ETNP) hosts the largest OMZ in the world, and its economic importance for the coastal regions of North and South America is indisputable (Levin, 2018). Numerous *in-situ* measurements during recurring oceanographic campaigns (e.g., CalCOFI, IMECOCAL; Lynn and Simpson, 1987; Bograd et al., 2003; Durazo-Arvizu and Gaxiola-Castro, 2010) revealed declining O<sub>2</sub> trends during the last few decades (Bograd et al., 2003, 2008; Lavin et al., 2013; Breitburg et al., 2018; Levin, 2018). It is important to note that some of the decreasing patterns could be biased by improvements in O<sub>2</sub> measurement technologies that have decreased minimum detection thresholds. Despite this caveat, high-resolution reconstructions of changes in dissolved oxygen in the ETNP OMZ over the past century yield contrasting observations, with warming and increasing extent of anoxia (<0.1 mL/L O<sub>2</sub>) not always correlated (Choumiline, 2011; Deutsch et al., 2014; Tems et al., 2016; Fu et al., 2018; Ontiveros-Cuadras et al., 2019). Ongoing discussions about the causes of OMZ intensification over the past decades typically invoke decreased O<sub>2</sub> solubility due to warming of the upper ocean, increased stratification slowing ventilation (Oschlies et al., 2008; Shaffer et al., 2009; Moffitt et al., 2015; Praetorius et al., 2015; Fu et al., 2018), and the strong effect of enhanced marine productivity on the formation of settling organic matter that undergoes decay and consumes more O<sub>2</sub> during remineralization (Wright et al., 2012; Levin, 2018). The latter relationship is the main mechanism by which some OMZ basins in the Eastern Pacific become anoxic (Moffitt et al., 2015; Breitburg et al., 2018; Levin, 2018). However, what causes increases in primary productivity is still debated, with initial results pointing to a complex interaction of factors involving increased upwelling rates and terrigenous discharge—both of which can provide the necessary nutrients for proliferation of primary producers (Howes et al., 2015).

Because the first analytical measurements of dissolved oxygen in seawater started in the late 1800s (Carpenter, 1965), data are not available for preceding portions of the nineteenth century. Nevertheless, multiple applications of well-established paleoceanographic proxies allow us to infer changes in earlier productivity and oxygenation by reconstructing past conditions preserved in the elemental composition of marine sedimentary records emphasizing organic carbon (C<sub>org</sub>), Ba, Cd, Mo, Mn, Ni, U, and V (Calvert and Pedersen, 1993; Helz et al., 1996; Morford and Emerson, 1999; Zheng et al., 2000; Lyons and Severmann, 2006; Tribovillard et al., 2006; Algeo and Rowe, 2012; Schoepfer et al., 2015). Multiple lines of proxy evidence show that major oxygenation shifts in the ETNP are coupled to glacial-interglacial cycling, often leading to a decrease in dissolved O<sub>2</sub> concentrations in North Pacific Intermediate and North Pacific Deep waters during glacial

stages (e.g., Last Glacial Maximum) as well as cold Dansgaard-Oeschger and/or Heinrich-like events (e.g., the Younger Dryas) (Ganeshram and Pedersen, 1998; Hendy and Kennett, 2000; Nameroff et al., 2004; Hendy and Pedersen, 2006; Tetard et al., 2017). Paleoceanographic changes are not only observed in sediment core records at OMZ-depths (400–1,000 m) but also in sediments collected at greater depths of the Pacific and shallower waters of the glacial Southern Ocean, which confirms the likelihood of widespread impacts on oxygenation far beyond intra-OMZ variability (Lu et al., 2016; Hoogakker et al., 2018). Important fluctuations of the upper OMZ also occurred. Rather than the traditional view of these fluctuations as lesser responses to minor climate perturbations, they may have dominated certain regions such as the ETNP. The Pacific Decadal Oscillation (PDO)—detected as decadal cyclic changes in climatic regime from warm to cold and vice versa—is one of these atmospheric effects with strong oceanographic implications (Mantua and Hare, 2002). The North Pacific Gyre Oscillation (NPGO) manifests in decadal fluctuations of nutrients, chlorophyll, and consequentially primary productivity that very often go hand to hand with atmospheric PDO changes in the Pacific (Di Lorenzo et al., 2008). Despite the similarities between the PDO and NPGO, they do not always co-vary.

High-resolution variability in paleoceanographic records, previously categorized by the scientific community as regional background noise, is now elucidating decadal- and centennial-scale OMZ fluctuations (Dean et al., 2004; Barron and Bukry, 2007; Choumiline, 2011; Deutsch et al., 2014; Tems et al., 2015, 2016). In the ETNP, cold PDO and/or NPGO phases cause intense upwelling off the western mainland of North America and lead to enhanced productivity, denitrification, and extreme water column anoxia (Di Lorenzo et al., 2008). However, numerous reports of marine sedimentary records in the literature typically lack the highly resolved age models needed to study decadal phenomena, which coupled with the absence of published multi-proxy records for denitrification ( $\delta^{15}\text{N}$ ) and water column redox (Cd, Mn, V, Mo, U) make ETNP-wide redox reconstructions challenging (Moffitt et al., 2015; Borreggine et al., 2017). The importance of reconstructing OMZ reoxygenation and deoxygenation events and mechanistically explaining their climatic causes is essential in light of current and potential future responses of the ocean to modern global warming. These efforts encounter further challenges as redox-sensitive data can be compromised when sediment cores from anoxic settings are not carefully sampled or stored with adequate care in core repositories (Zheng et al., 2000; McManus et al., 2006; Scholz et al., 2011; Costa et al., 2018).

Here we reconstruct changes in the ETNP OMZ based on sediment cores collected at various depths in the Gulf of California. To achieve an ETNP-wide reconstruction, we integrate our multiproxy record of paleoproductivity and paleoredox with published sediment cores from the region. Further, to avoid misinterpreting local variability as global patterns, we apply geostatistical and numerical approaches to existing datasets to unmix local from larger-scale controls.

## Strengths and Weaknesses of Geochemical Proxies as Applied to Oxygen Minimum Zone Reconstructions

In this section we provide background details for productivity and redox proxies as archived in marine sediments and as applied to OMZ reconstructions.

### Productivity Proxies ( $C_{org}$ , $Ba_{excess}$ , Ni)

Organic carbon ( $C_{org}$ ) has long been used as a proxy for exported organic matter because of its analytical simplicity and wide range of applications (Schoepfer et al., 2015). While  $C_{org}$  could directly represent superficial primary productivity, this possibility is likely confounded by multiple controls on remineralization and burial that are tightly related to reactivity of organic matter, bioturbation, and oxygen availability (Calvert et al., 1996; Burdige, 2007; Bianchi et al., 2016).

Barite, Ba/Al, and excess barium ( $Ba_{excess}$ ) have been used widely as productivity proxies (Dymond et al., 1992; Eagle et al., 2003; Anderson and Winckler, 2005; Schoepfer et al., 2015), although barite and  $Ba_{excess}$  relationships with productivity may be complicated by post-burial reprecipitation (McManus et al., 1998; Riedinger et al., 2006; Schoepfer et al., 2015). In some well-oxygenated marine settings, sedimentary  $Ba_{excess}$  corresponds well to changes in productivity established by other proxies (e.g., Ni, P, and biogenic silica) (Schoepfer et al., 2015). However, post-depositional diagenetic remobilization of Ba has been found both in regions with transient anoxia and where bottom waters are well-oxygenated (McManus et al., 1998; Riedinger et al., 2006; Schoepfer et al., 2015). Sedimentary records of  $Ba_{excess}$  can be further compromised over glacial-interglacial cycles when significant reoxygenation can cause redissolution and reprecipitation of barite along reaction fronts (McManus et al., 1998; Riedinger et al., 2006; Schoepfer et al., 2015).

Nickel is actively involved in biological cycling related to diatom export (Dupont et al., 2010; Twining et al., 2012). Dissolved Ni is removed from the water column by organic matter and supplied to the bottom sediments through particle settling (Böning et al., 2015). In sediments, Ni is the best-known analog for fresh organic matter because it mirrors the input of chlorins—one of the degradation products of chlorophyll (Böning et al., 2015). An advantage of Ni over other biologically active trace elements is its detachment from Mn and S cycling, compared to Cd and Zn, which more readily form insoluble sulfides (Morse and Luther, 1999; Böning et al., 2015). Potential complications for Ni as a productivity proxy include its elevated concentration in the detrital fraction (Wedepohl, 1995) and the possibility of anthropogenic contribution of Ni to marine sediments (Reck et al., 2008).

### Redox Proxies (Mo, Cd, V, U)

Molybdenum enrichment processes are linked with incorporation into pyrite and associations with organic matter, which often require abundant hydrogen sulfide (Calvert and Pedersen, 1993; Tribouillard et al., 2008; Chappaz et al., 2014; Scholz et al., 2017). An important pathway for Mo enrichment is the transformation of molybdate to thiomolybdates ( $MoO_xS_{4-x}^{2-}$ , where  $x = 0 \sim 4$ ), which are highly particle reactive (Helz et al.,

1996; Erickson and Helz, 2000; Scholz et al., 2017). Additionally, Mo can be scavenged by Fe-Mo-S clusters (Helz et al., 2011) or adsorbed onto sulfide-rich organic matter (Helz et al., 1996). Molybdenum enrichments can occur diagenetically (within the sediments), in the water column, or in some cases near the sediment-water interface, which was reported for OMZs (Zheng et al., 2000). While widely used as an indicator of past anoxic and euxinic (anoxic and sulfidic) conditions, several complications have been reported for this proxy (Morford and Emerson, 1999; Chappaz et al., 2014), including localized Mo enriched in turbidites despite fully oxygenated water column conditions (McKay and Pedersen, 2014) and uptake exclusively within the sediments when significant amounts of sulfide are present solely in pore waters (Zheng et al., 2000; Scholz et al., 2017; Hardisty et al., 2018)—although these enrichments tend to fall below those typical of euxinic settings (e.g., Scott and Lyons, 2012).

Cadmium is a biologically active trace element supplied to marine sediments in association with organic matter (Morford and Emerson, 1999). It has been used as a proxy for strongly reducing waters (Calvert and Pedersen, 1993; Tribouillard et al., 2006). Cadmium can be precipitated in the presence of  $H_2S$ , which makes it a particularly good indicator of euxinia (Morse and Luther, 1999).

Vanadium is present in well-oxygenated seawater in its V(+5) form, usually as  $H_2VO_4^-$ , which is reduced to V(+4) as  $VO^{2+}$  under oxygen-deficient conditions (Calvert and Pedersen, 1993; Morford and Emerson, 1999). This V(+4) form is more effectively scavenged and can be adsorbed to Fe-(oxyhydr)oxides, which is one of its removal mechanisms from seawater (Bauer et al., 2017; Ho et al., 2018). Over sub-millennial and glacial-interglacial timescales, V is potentially one of the most reliable redox proxies, tightly following changes in oxygenation (Nameroff et al., 2004; Costa et al., 2018). The contribution of non-lithogenic V through particulate settling has not been fully constrained; however, slight enrichments in suspended and settling matter have been found (Rodríguez-Castañeda, 2008; Hakspiel-Segura et al., 2016; Bauer et al., 2017; Ho et al., 2018; Conte et al., 2019).

Uranium is widely used as paleoredox proxy; however, the pathways of its sedimentary enrichment are still not fully understood. Uranium is present in seawater in the dissolved U(+6) form as uranyl carbonate complexes ( $UO_2^{2+}$ ) that are reduced under anoxic conditions to the insoluble U(+4) form by inorganic and microbially mediated processes (Ku et al., 1977; Klinkhammer and Palmer, 1991; Dunk et al., 2002) resulting in the formation of solid particles. Uranium can also be adsorbed to organic matter and to Fe- and Mn-(oxyhydr)oxides (Anderson et al., 1989). While increases in particulate U are thought to mostly occur diagenetically in sediment pore waters underlying strongly anoxic and sulfidic (euxinic) waters (Klinkhammer and Palmer, 1991), some particulate non-lithogenic U can form very slowly in the water column (Zheng et al., 2002; Holmden et al., 2015). The extent to which non-lithogenic U can be enriched in marine particles is not well-established and may be more common in highly productive OMZ-type settings than previously thought. We propose an updated model for the behavior of U in OMZs, which will be discussed further in the paper.

## METHODS

### Depositional Setting

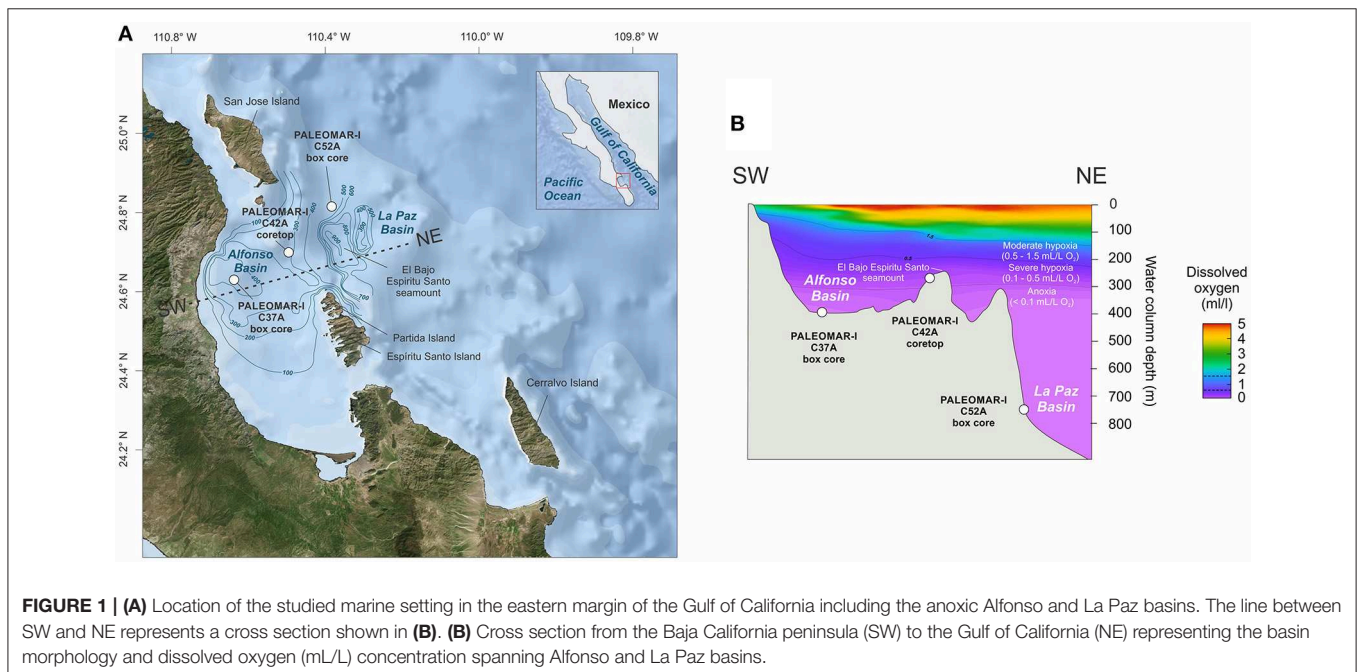
The Gulf of California (GC) is located within the ETNP OMZ and is well-connected to the Eastern Pacific through its southern entrance (Lavín et al., 2013). Circulation is not known to be limited in most GC basins, including Guaymas, Pescadero, and La Paz. Alfonso Basin is the only partially restricted setting in the GC, with a bathymetric sill extending today to a depth of 250 m (Nava-Sánchez et al., 2001). The sill restricts the incursion of North Pacific Intermediate Water (NPIW) and North Pacific Deep Water (NPDW) (Figures 1A,B). Primary productivity is higher on the eastern side of the GC because it is nourished by nutrients upwelled predominantly during dry and cold seasons with strong northwesterly winds (Lavín et al., 2013; Silverberg et al., 2014). Mesoscale eddies together with wind-driven coastal upwelling (primarily along the mainland margin during winter) promote primary productivity in the region (Badan-Dangon et al., 1991; Trasviña-Castro et al., 2003; Deutsch et al., 2014). A strong east-to-west gradient persists from autumn through spring (Lavín et al., 2013), which results in organic material produced in the upwelling system on the eastern margin being deposited as biogenic remains on the west side of the basin.

Particularly in Alfonso Basin, productivity is regulated by cyclonic flow that produces water divergence—transporting nutrients from the subsurface waters (>60 m) into the photic zone. This cyclonic gyre is semi-permanent and has been linked by past researchers to the increase in productivity (Monreal-Gómez et al., 2001; Coria-Monter et al., 2014). Satellite and *in-situ* measurements of Net Primary Productivity (NPP) in Alfonso Basin range from 0.5 to 3.5 gC m<sup>-2</sup>d<sup>-1</sup> over the last decade and show an inverse correlation with surface temperature.

Mesoscale transport processes explain why the Gulf of California, like most of the Eastern Pacific, is influenced by ENSO, PDO, and/or NPGO phenomena (Mantua and Hare, 2002; Di Lorenzo et al., 2008). During cold La Niña years, the Walker Circulation triggers upwelling and productivity in the Eastern Pacific—weakening the typical upper ocean stratification that dominates during normal and El Niño years (Thunell, 1998; McPhaden, 2004; Bustos-Serrano and Castro-Valdez, 2006). Atmospheric circulation is also an important mechanism that seems to control upwelling in the Gulf of California and is dictated by the North American Monsoon (NAM) (Metcalf et al., 2015). When the North Pacific High (NPH) and the Intertropical Convergence Zone (ITCZ) migrate southward, intense upwelling is triggered by northwesterly winds (Schneider et al., 2014; Metcalf et al., 2015; Staines-Urías et al., 2015). Longer-scale variability of similar nature is attributed to cold PDO and sometimes NPGO phases, but the atmospheric and oceanographic links are still unclear.

The water columns of Alfonso and La Paz basins show a pronounced decrease in oxygen with depth, reaching values below 0.1 mL/L O<sub>2</sub> (Figure 1B). To avoid the imprecise term “suboxic” (Canfield and Thamdrup, 2009), we classify the water column using the threshold O<sub>2</sub> values from Hofmann et al. (2011) and Moffitt et al. (2015), which yielded the following categories: oxic ([bottom O<sub>2</sub>] > 1.5 mL/L), moderately hypoxic (0.5 mL/L < [bottom O<sub>2</sub>] < 1.5 mL/L), severely hypoxic (0.1 mL/L < [bottom O<sub>2</sub>] < 0.5 mL/L), and anoxic ([bottom O<sub>2</sub>] < 0.1 mL/L). According to this classification, both Alfonso and La Paz basins fall within the “anoxic” category (Figure 1B).

Due to their locations near the open Pacific Ocean, the southern basins are a sensitive recorder of regional variation in the GC and the larger-scale climate circulation of the ETNP,



capturing changes in productivity and redox conditions useful for tracking fluctuations of the OMZ (Dean et al., 2004; Barron and Bukry, 2007; Dean, 2007; Pérez-Cruz, 2013; Deutsch et al., 2014; Tems et al., 2015, 2016; Ontiveros-Cuadras et al., 2019).

## Sampling

Laminated sediments from marine basins of the Gulf of California with varying degrees of deoxygenation were collected using a Reineck box corer during the PALEOMAR-I campaign in November 2014 aboard R/V “El Puma” owned by UNAM, Mexico (Figures 1A,B). The 50 cm sediment core PALEOMAR-I C37A was collected at 408 m water depth in the silled Alfonso Basin. Core PALEOMAR-I C52A represents a sedimentary sequence of the upper 24 cm of La Paz Basin at 785 m depth. Both cores show a clear, continuously laminated fabric. Additionally, the core top of PALEOMAR-I C42A was sampled from the shallower part of Alfonso Basin (265 m). This core did not show clear laminations. Poor recovery during retrieval limited its utility for paleoceanographic reconstructions. From this point forward, we will refer to these cores as C37A, C42A, and C52A.

Each core was extruded and subsampled immediately after collection, and pore waters were extracted from each section in a glove bag under N<sub>2</sub> atmosphere using CSS 5 cm Rhizon samplers attached to plastic syringes (Lyons and Berner, 1992; Dickens et al., 2007; Raiswell and Canfield, 2012; Riedinger et al., 2017). Each core segment yielded approximately 8 mL of pore waters, which were filtered at 0.2 μm, acidified with trace grade pure nitric acid (10 μL of acid per each 1 mL of sample), and stored at 4°C (Riedinger et al., 2014, 2017). Prior to analysis, solid-phase samples were dried, weighed, and homogenized.

## Age Model

We use the present-day sedimentation rates previously reported in the literature for Alfonso Basin to generate the age model for the studied core C37A. Due to the extended timespan of the sedimentary section, the composite age model is based on <sup>210</sup>Pb and <sup>14</sup>C dating methods (Figure 2; Table 1). For this purpose, we selected box core DIPAL-II C44 (Choumiline, 2011) and gravity core DIPAL-III T43 (Pérez-Cruz, 2013). The dated materials were collected at the same location within the basin and span a matching sedimentary package (Supplementary Figure 1). High-resolution sections of the uppermost 10 cm (subsampled at <3 mm) of core DIPAL-II C44 were analyzed for <sup>210</sup>Pb at Flett Research Ltd. Laboratory (Winnipeg, Canada) (Supplementary Figure 2). The mean sedimentation rate for the upper 10 cm is 0.61 mm/year in Alfonso Basin (Choumiline et al., 2010; Choumiline, 2011). The sedimentary section of the gravity core DIPAL-III T43 corresponding to the lower part of C37 (between 15 and 50 cm) was dated using the <sup>14</sup>C method (Pérez-Cruz, 2013). Measurements were performed in benthic foraminifera *Bolivina subadvena* by accelerator mass spectrometry at Beta Analytic (Pérez-Cruz, 2013) and the radiocarbon values were calibrated using the Marine13 curve (Reimer et al., 2013). This part of the core yielded a mean sedimentation rate of 0.8 mm/year (Pérez-Cruz, 2013). In our age model for C37A we extrapolate the sedimentation rate of 0.61 mm/year to the

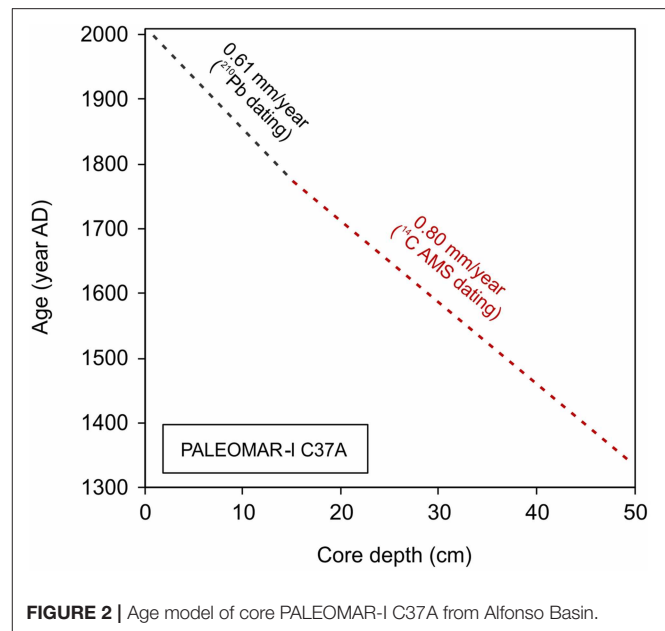


FIGURE 2 | Age model of core PALEOMAR-I C37A from Alfonso Basin.

uppermost core section (0–15 cm) and use 0.8 mm/year for the lowermost segment (15–50 cm) as shown in Table 1 and Supplementary Figure 1. To demonstrate that the core sections are equivalent, we compared the total carbon ( $C_{tot}$ ), calcium carbonate ( $CaCO_3$ ) and Ca changes through time for cores C37A (this study), DIPAL-II C44 (Choumiline et al., 2010, 2017; Choumiline, 2011) and DIPAL-III T43 (Pérez-Cruz, 2013). The curves covary, confirming the consistency between age models for different core records (Supplementary Figure 1). Additionally, selected dry splits of sediment core C37A (Alfonso Basin) were dated using the <sup>210</sup>Pb and <sup>137</sup>Cs methods via gamma-ray spectroscopy in the Gray Lab (University of California, Riverside). The subsampling resolution of this core was too coarse to produce a robust age model using these methods. Despite known difficulties with radiocesium detection in the region (Ruiz-Fernández et al., 2009) it was still possible to find slightly elevated <sup>137</sup>Cs activity values around the 2–4 cm core horizon, very likely corresponding to the mid-1960s peak of nuclear testing in the atmosphere (Foster and Walling, 1994). The resulting linear sedimentation rate using the radiocesium method for core C37A was roughly 0.6 mm/year. The sedimentation rates determined for Alfonso Basin from different age models are consistent. Further, the age model for Alfonso Basin shows that the deepest sample of core C37A at 50 cm extends to 1300 AD (also called the Common Era or CE).

## Analytical Approaches

Total carbon ( $C_{tot}$ ) and total inorganic carbon ( $C_{inorg}$ ) in dry sediment subsamples were measured on an ELTRA CS-500. The CO<sub>2</sub> produced during subsample combustion at 1350°C ( $C_{tot}$ ) or acidification with 20% HCl ( $C_{inorg}$ ) was quantified with an infrared analyzer. The organic carbon ( $C_{org}$ ) fraction was calculated by numerical difference:  $C_{org} = C_{tot} - C_{inorg}$ .

**TABLE 1** | Age model for core C37A, constructed by a combination of extrapolated average sedimentation rates produced using the  $^{210}\text{Pb}$  method on core DIPAL-II C44 (Choumiline et al., 2010; Choumiline, 2011) and acceleration mass spectrometry  $^{14}\text{C}$  on core DIPAL-III T43 (Pérez-Cruz, 2013).

Depth range (cm)	Depth midpoint (cm)	Age in years AD	Dated material and method used	Corresponding sedimentation rate for C37A
0–2	1	1999	$^{210}\text{Pb}$ dating of the	0.61 mm/year
2–4	3	1967	uppermost 10 cm of bulk	
4–6	5	1934	sediment from box core	
6–8	7	1902	DIPAL-II C44	
8–10	9	1870		
10–12	11	1837		
12–14	13	1805		
14–16	15	1772		0.8 mm/year
16–18	17	1747	AMS $^{14}\text{C}$ dating with	
18–20	19	1722	<i>Bolivina subadvena</i> in the	
20–22	21	1697	following horizons of the	
22–24	23	1672	gravity core DIPAL-III T43:	
24–26	25	1647	Code: BETA320950	
26–28	27	1622	Interval: 17–18 cm	
28–30	29	1597	Age: 1572 year AD	
30–32	31	1572		
32–34	33	1547	Code: BETA322689	
34–36	35	1522	Interval: 41–43 cm	
36–38	37	1497	Age: 1240 year AD	
38–40	39	1472		
40–42	41	1447		
42–44	43	1422		
44–46	45	1397		
46–48	47	1372		
48–50	49	1347		

The cores were collected at the same location in Alfonso Basin.

Prior to sample digestion, 100 mg splits were ashed in ceramic vessels for 8 h at 550°C in a high temperature oven. A two-step digestion procedure involved a mixture of  $\text{HNO}_3$  and HF, followed by aqua regia (HCl and  $\text{HNO}_3$ ) and acidification/drying cycles on temperature-controlled hot plates. A very low HF: $\text{HNO}_3$  ratio of 1:8 was employed during the first step to prevent insoluble fluoride formation. Careful evaluation of each sample revealed that no undissolved particles were detected, suggesting complete digestion (Durand et al., 2016). The final digested extracts were diluted in 2%  $\text{HNO}_3$  and measured for major and trace elements (Al, Ba, Cd, Fe, Ni, Mo, V, U) on an Agilent 7900 Inductively Coupled Mass Spectrometer (ICP-MS).

Pore waters were analyzed for elemental composition on an Agilent 7900 ICP-MS, emphasizing dissolved Fe, Mn, and selected trace elements. The quality of our data was assessed by analyzing duplicates and certified reference materials USGS SGR-1B, USGS SDO-1, NIST 2702, AR4007, and AR4024. Analytical precision was always below 3%. Recoveries of measured sample relative to certified standard value ranged between 96 and 105%.

## Numerical and Statistical Approaches

The productivity and redox proxy approaches used here rely heavily on authigenic enrichment of trace elements relative

to detrital inputs through uptake in marine sediments during diagenesis and via scavenging from seawater during primary production and during particle settling. To assess enrichments relative to detrital contributions, each element was normalized to Al as a reliable crustal proxy (Wedepohl, 1995). Further, to account for dilution by  $\text{CaCO}_3$ , which can cause apparent elemental variability, we recalculated the data on a carbonate free basis (CFB) by dividing each concentration by the fraction of non-carbonate material. Elemental ratios were also calculated for selected elements. The authigenic uranium ( $U_{\text{auth}}$ ) fraction was calculated as  $U_{\text{auth}} = U_{\text{total}} - (\text{Th}/3)$  (Wignall and Myers, 1988).

Due to limited sample sizes, it was not possible to perform the barite sequential leach sometimes used as a productivity proxy in well-oxygenated marine settings (Dymond et al., 1992; Eagle et al., 2003; Schoepfer et al., 2015). Instead, we used our measurements for total Ba and Al to determine excess barium ( $\text{Ba}_{\text{excess}}$ ) as the closest calculated alternative (Eagle et al., 2003; Anderson and Winckler, 2005):  $\text{Ba}_{\text{excess}} = \text{Ba}_{\text{total}} - (\text{Ba}_{\text{terrigenous}}/\text{Al}_{\text{terrigenous}}) \times \text{Al}_{\text{total}}$ . We assumed a  $\text{Ba}_{\text{terrigenous}}/\text{Al}_{\text{terrigenous}}$  ratio of 0.0045 as suggested by Dymond et al. (1992) and Eagle et al. (2003).

In order to define proxy associations, we applied a multivariate statistical approach for the proxy datasets from Alfonso and La

Paz basins. Specifically, we performed R-mode Factor Analysis with Varimax rotation using the software STATISTICA by StatSoft. The analysis included the following variables:  $C_{org}$ ,  $Ba_{excess}$ , Ni, U,  $U_{auth}$ , Cd, Mo, and V.

Geostatistical analyses and data extraction techniques were performed using ArcGIS 10.6 software by ESRI. We combined our data with previously published geochemical records obtained in part from the EarthChem SedDB database via the Interdisciplinary Earth Data Alliance (IEDA) repository. Estimated oceanographic data (dissolved  $O_2$  and chlorophyll) were obtained for each core location in GIS and used in our statistical analysis. Global oceanic oxygen data are based on the World Ocean Atlas (2005) and Garcia et al. (2006); surficial chlorophyll estimates from the SeaWiFS satellite sensor were published by OBP/NASA.

## Paleoceanographic Proxies Used in This Study

To interpret past OMZ conditions preserved in marine sediments we used a combination of proxies assuming  $C_{org}$  as an indicator for organic carbon burial (Schoepfer et al., 2015);  $Ba_{excess}$  (despite the caveats described above) and Ni for export production (Böning et al., 2015; Schoepfer et al., 2015); Cd, Mo, and V for bottom water anoxia (Calvert and Pedersen, 1993; McManus et al., 2006; Tribovillard et al., 2006; Lyons et al., 2009). Due to a strong contribution of  $U_{auth}$  via settling particulates (Choumiline et al., 2010; Choumiline, 2011) potentially after its reduction or adsorption to organic matter, this proxy could trace both redox and productivity—as will be explained further in the paper.

While each proxy has distinct biogeochemistry and enrichment pathways, they are all affected by a circular relationship between productivity and redox (Tribovillard et al., 2006; Schoepfer et al., 2015; Bianchi et al., 2016). In transiently anoxic settings high productivity often leads to the development of water column anoxia, which favors organic preservation and reduces the mobility of productivity proxies (Schoepfer et al., 2015). Due to the latter, it is often common to expect a covariance between productivity and redox proxies (Tribovillard et al., 2006; Bianchi et al., 2016). The differences in proxy relationships are often helpful to unravel more specific biogeochemical processes tied to preservation biases, such as organic matter reactivity and post-depositional diagenetic transformations.

## RESULTS AND DISCUSSION

### Geochemistry of Modern Sediments From the Southwestern Gulf of California at Various OMZ Depths

The chemical compositions of core tops (upper 2 cm) represent the most recent sediments from Alfonso and La Paz basins (Table 2). A water depth transect from the 265 to 785 m through the study region revealed that dissolved  $O_2$  values decreased from 0.3 mL/L (uppermost OMZ) to <0.1 mL/L (OMZ core) (Figure 1B). Most redox-sensitive elements increase in concentration in the deeper sites C37A and C52A relative to the

shallower C42A. For all three sites the elemental concentrations range as follow:  $C_{org}$  (2.96–6.41%),  $Ba_{excess}$  (175.50–682.77 mg/kg), Ni (26.84–49.06 mg/kg), and Mo (0.75–6.75 mg/kg). In contrast, Cd and  $U_{auth}$  are enriched at the shallow, more oxygenated site C42A—reaching 13.17 mg/kg for Cd and 5.34 mg/kg for  $U_{auth}$ , compared to 7.24 mg/kg for  $U_{auth}$  in C52A and 2.48 mg/kg for Cd in C37A (Table 2). Although circulation in Alfonso Basin is slightly restricted due to the presence of a bathymetric sill at 250 m depth, restriction was apparently not severe enough to limit trace element enrichments in La Paz Basin relative to the more open ocean. We calculated  $U_{auth}$  values for the CFB fraction as 6.43 mg/kg in C42A, 7.26 mg/kg in C37A, and 7.24 mg/kg in C52A. Carbonate-free values were also calculated for the other proxies but did not produce major differences relative to either total or Al-normalized data (see Supplementary Material).

### Bioturbation and Post-sampling Effects as Complicating Overprints on Primary Proxy Records

Visual observation confirmed that the sediments from Alfonso (C37A) and La Paz (C52A) basins are clearly laminated, with no evidence for bioturbation, which could obscure primary sedimentary features. Pore water profiles were used to establish the chemical zonation of electron acceptors at the time of sample collection (Canfield and Thamdrup, 2009). It is essential to evaluate diagenetic conditions before applying paleoreconstruction techniques because many proxies can be overprinted during diagenesis, obscuring records of primary water column conditions (Calvert and Pedersen, 1993; Tribovillard et al., 2006). Further, pore water data shed light on bioturbational overprints via burrow irrigation and sediment homogenization and disturbance during sediment collection and processing. At both Alfonso Basin (C37A) and La Paz Basin (C52A), concentrations of dissolved Fe ( $Fe_{diss}$ ) and dissolved Mn ( $Mn_{diss}$ ) show downcore decreases (Figure 3). The observed trend for  $Fe_{diss}$  is similar to those from analogous OMZ settings of the Gulf of California (Guaymas Basin), offshore California (San Pedro and Catalina basins), and the Peruvian margin—that is, pore water  $Fe_{diss}$  reaches its maximum a few centimeters below the sediment-water interface and gradually declines down core (Brumsack and Gieskes, 1983; McManus et al., 1997; Canfield and Thamdrup, 2009; Scholz et al., 2011; Scholz, 2018). Our recovery of expected trends suggests that proper techniques for sediment collection and preservation were employed in this study.

### Downcore Records of Changing Productivity and Redox

Here we present downcore variations of productivity and redox proxies recorded in our sedimentary material from the ETNP (Figure 1). We found almost no difference between the trends for absolute concentrations and corrected data, so we present only absolute values. However, Al-normalized and CFB data are presented in Supplementary Materials for the interested reader.

**TABLE 2** | Composition of modern sedimentary material represented by core tops from different OMZ depths in Alfonso (C42A and C37A) and La Paz basin (C52A).

Marine basin	Water column depth	Redox condition and bottom dissolved O <sub>2</sub> (mL/L)	Core top proxy data							
			Productivity/nutrients			Redox and/or Productivity			Redox	
			C <sub>org</sub> (%)	Ba <sub>excess</sub> (mg/kg)	Ni (mg/kg)	U (mg/kg)	U <sub>auth</sub> (mg/kg)	Cd (mg/kg)	Mo (mg/kg)	V (mg/kg)
Alfonso Basin (C42A)	Uppermost OMZ (265 m)	Severe hypoxia (~0.3)	2.96	175.70	26.84	14.31	13.17	5.34	0.75	26.05
Alfonso Basin (C37A)	Upper OMZ (408 m)	Anoxia (<0.1)	6.01	406.37	40.25	9.85	8.14	2.48	6.34	124.67
La Paz Basin (C52A)	Middle OMZ (785 m)	Anoxia (<0.1)	6.41	682.77	49.06	8.84	7.24	2.60	6.75	75.048

The dissolved oxygen values presented here were obtained during the PALEOMAR-I oceanographic campaign.

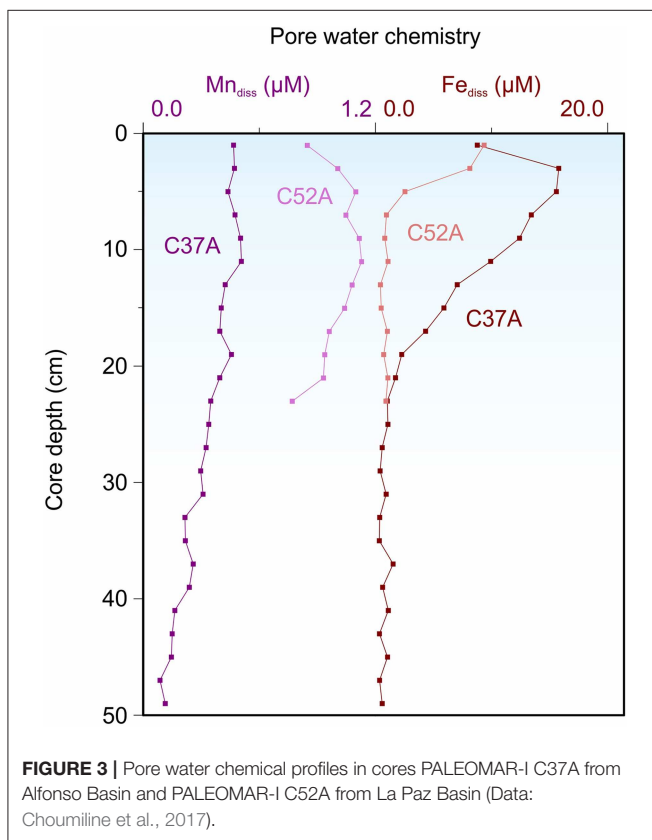


**FIGURE 3** | Pore water chemical profiles in cores PALEOMAR-I C37A from Alfonso Basin and PALEOMAR-I C52A from La Paz Basin (Data: Choumiline et al., 2017).

### Geochemistry of Sediments From the Upper OMZ in Alfonso Basin

Elemental profiles for C37A from Alfonso Basin are shown in **Table 3**. Data for C<sub>org</sub> are in good agreement with Ba<sub>excess</sub>, Ni, U<sub>auth</sub>, and V as proxies for past oxygenation and/or primary productivity. Values range from 5.60 to 6.76% for C<sub>org</sub>, 372.22–491.54 mg/kg for Ba<sub>excess</sub>, 40.25–51.61 mg/kg for Ni, 9.23–14.15 mg/kg for U, 7.71–12.48 mg/kg for U<sub>auth</sub>, and 115.81–172.40 mg/kg for V. Trends for Cd and Mo differ slightly from those

for the other proxies and range from 2.48 to 7.04 mg/kg and 6.34–15.16 mg/kg, respectively (**Figure 4**).

### Geochemistry of Sediment From the Mid-Depth OMZ of La Paz Basin

Downcore concentrations for the productivity and redox proxies in core C52A from La Paz Basin are presented in **Table 3**. Despite differences in core length and depositional setting, the records for C<sub>org</sub>, Ni, U<sub>auth</sub>, V, and Cd in C52A are similar to those from core C37A (**Supplementary Figure 3**). These elements range as follow: 6.51–7.12% for C<sub>org</sub>, 47.34–53.25 mg/kg for Ni, 5.97–9.32 mg/kg for U<sub>auth</sub>, and 74.31–102.80 mg/kg for V. In C52A, Ba<sub>excess</sub> does not covary with Ni and U<sub>auth</sub>, pointing to its potential remobilization during diagenesis. Excess-Ba concentrations range from 419.76 to 763.24 mg/kg but are mostly uniform over the length of the core—averaging 670.89 mg/kg. The trends for Cd and Mo decrease down core in the upper 6 cm of laminated sediments (**Supplementary Figure 3**; **Table 3**) and range from 2.38 to 2.97 and 4.90 to 12.55 mg/kg, respectively.

The lowest concentrations for most proxy data are found in the upper 5 cm, at ~14 cm, and below 23 cm—perhaps corresponding to well-ventilated past conditions. The highest values, indicating enhanced anoxia, were registered around 20 cm for all proxies, while the second anoxic horizon close to 10 cm was only captured by C<sub>org</sub>, Ni, U<sub>auth</sub>, V, and more subtly by Cd and Mo.

### Variability of the Upper OMZ in Alfonso Basin Over the Last 700 Years

We present down-core elemental concentrations in the context of the age model described earlier in the paper. Due to multiple challenges during our efforts to date cores C42A and C52A, such as poor recovery, only core C37A from Alfonso Basin produced a robust age model. Core C37 will be emphasized for paleoceanographic reconstructions for the remainder of the report.

The geochemical profiles for C37A from Alfonso Basin record changes in the upper OMZ boundary dating back to 1300 AD

**TABLE 3** | Elemental composition of the solid phase from cores C37A, C42A, and C52A collected during PALEOMAR-I expedition to the Gulf of California.

Core	Depth range (cm)	C <sub>org</sub> (%)	Al (%)	Fe (%)	Ba (mg/kg)	Cd (mg/kg)	Mo (mg/kg)	Ni (mg/kg)	U (mg/kg)	V (mg/kg)	Ba <sub>excess</sub> (mg/kg)	U <sub>auth</sub> (mg/kg)
C37A (Alfonso Basin)	0–2	6.01	4.9	2.5	406.4	2.5	6.3	40.3	9.9	124.7	406.4	8.1
	2–4	6.18	5.1	2.6	419.3	2.6	6.4	41.9	10.1	115.8	419.2	8.3
	4–6	6.13	5.1	2.6	440.0	3.4	9.3	41.3	9.7	133.4	439.9	7.9
	6–8	6.42	5.0	2.5	454.3	3.4	10.2	44.2	10.1	137.1	454.3	8.4
	8–10		4.7	2.3	439.9	3.5	9.9	44.0	11.3	139.6	439.9	9.6
	10–12	6.39	4.8	2.3	430.4	3.8	9.0	45.3	13.0	150.6	430.4	11.3
	12–14	6.65	5.0	2.5	476.6	4.1	9.5	47.9	13.5	156.8	476.6	11.7
	14–16	6.66	5.3	2.6	479.3	3.8	9.2	48.3	12.4	141.8	479.3	10.6
	16–18	6.76	4.3	2.1	416.0	3.8	9.2	41.2	9.2	117.0	415.9	7.7
	18–20	6.26	4.9	2.4	458.0	3.9	8.7	45.8	11.6	149.7	458.0	9.9
	22–24	6.43	5.0	2.6	480.5	4.8	12.7	49.5	10.9	167.1	480.5	9.1
	24–26	6.05	4.8	2.4	458.3	4.6	11.2	46.3	12.9	157.0	458.3	11.2
	26–28	6.56	4.9	2.4	459.1	4.7	8.2	50.4	12.4	154.9	459.1	10.7
	28–30	6.25	5.0	2.5	461.5	5.4	13.4	46.9	10.8	160.0	461.4	9.0
	30–32	5.93	5.0	2.5	485.5	5.0	13.0	46.4	11.2	164.2	485.5	9.5
	32–34	5.89	4.9	2.5	468.1	4.8	11.2	47.7	11.8	160.6	468.1	10.1
	34–36	6.53	5.1	2.6	488.8	5.3	12.9	51.6	11.9	172.4	488.7	10.1
	36–38	6.18	5.1	2.5	470.3	4.3	10.7	48.9	11.1	167.5	470.3	9.4
	38–40	6.04	5.1	2.5	441.8	3.7	9.3	46.1	11.3	146.4	441.8	9.5
	40–42	6.30	5.1	2.5	472.7	4.7	13.5	48.9	10.1	161.0	472.7	8.3
42–44	6.65	4.7	2.4	481.5	7.0	14.2	51.4	14.2	170.8	481.5	12.5	
44–46	5.60	4.6	2.4	372.2	2.9	6.8	42.8	14.0	124.0	372.2	12.3	
46–48	6.62	4.6	2.3	440.1	5.0	13.3	46.3	9.9	148.5	440.1	8.2	
48–50		4.8	2.4	491.6	5.2	15.2	50.0	12.9	165.9	491.5	11.2	
C52A (La Paz Basin)	0–2	6.41	4.3	1.8	682.8	2.6	6.7	49.1	8.8	75.0	682.8	7.2
	2–4	6.58	4.3	1.9	681.1	2.4	4.9	49.4	7.5	76.0	681.1	6.0
	4–6	6.55	4.3	1.9	419.8	2.5	9.1	49.0	8.3	76.5	419.8	6.8
	6–8	6.68	4.3	1.9	580.4	2.5	10.7	49.9	8.4	86.8	580.4	6.8
	8–10	7.12	4.6	1.9	763.3	3.0	12.6	52.9	9.7	102.8	763.2	8.1
	10–12	6.61	4.4	1.8	689.6	2.8	11.8	50.7	10.4	93.4	689.5	8.8
	12–14	6.43	4.4	1.9	704.3	2.8	10.6	49.9	9.2	88.4	704.3	7.6
	14–16	6.54	4.6	1.9	723.0	2.8	9.9	51.7	9.6	83.9	722.9	8.0
	16–18	6.40	4.6	1.9	703.2	2.9	9.6	51.1	8.8	80.9	703.2	7.2
	18–20	6.49	4.8	2.0	728.1	2.9	10.3	53.2	11.1	94.7	728.1	9.3
	20–22	6.17	4.3	1.9	661.3	2.7	9.5	47.3	8.6	82.2	661.3	7.0
22–24	6.10	4.5	2.0	714.1	2.4	10.9	50.2	9.1	74.3	714.1	7.5	
C42A	-	2.96	2.3	1.0	175.7	5.3	0.8	26.8	14.3	26.0	175.7	13.2

(Figure 4; Table 3). Data for C<sub>org</sub> are in good agreement with Ba<sub>excess</sub>, Ni, U<sub>auth</sub>, and V as proxies for past oxygenation and/or primary productivity. Unlike our other proxies, Mo and Cd remain high from 1300 to 1700 AD and then slowly transition toward lower values after 1700 AD. This slight decrease toward the present corresponds to the uppermost 20 cm of the record in the Alfonso Basin. The lowest concentrations for our proxies are generally concurrent with the late 1900s, early 1700s, and late 1300s AD. These times correspond to warm periods of the past millennium as reconstructed by multiple records (IPCC, 2014), including the anthropogenically caused warming trend that started around the beginning of the nineteenth century and extends to present day (Figure 4). Lower proxy values indicate

decreased primary productivity and correspond to slightly more oxygenated times. In contrast, high proxy values occurred in the early 1800s, late 1600s, early 1500s, and early 1400s, with maxima between roughly 1700 and 1400 AD are likely associated with the prolonged cold period of the Little Ice Age. Higher values usually correspond to increased primary productivity in surface waters and enhanced anoxia.

### Multivariate Statistical Associations of Paleoproxies in Alfonso and La Paz Basins

Factor analysis results for the combined geochemical datasets from Alfonso Basin (core C37A) and La Paz Basin (C52A) distinguished three elemental associations between Factor 1

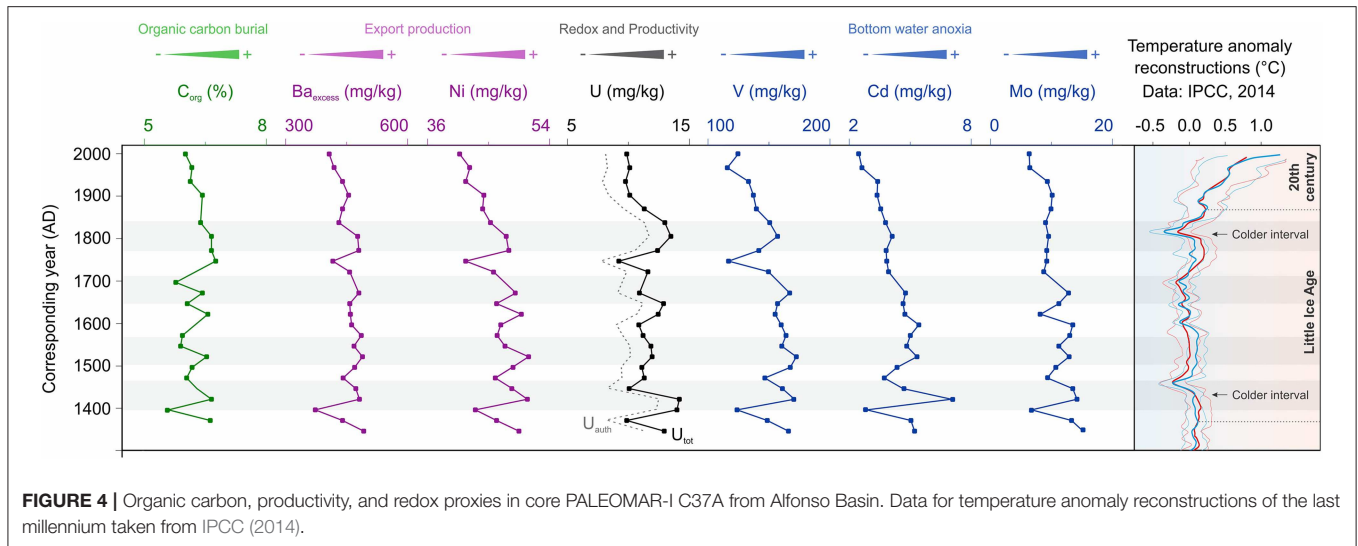


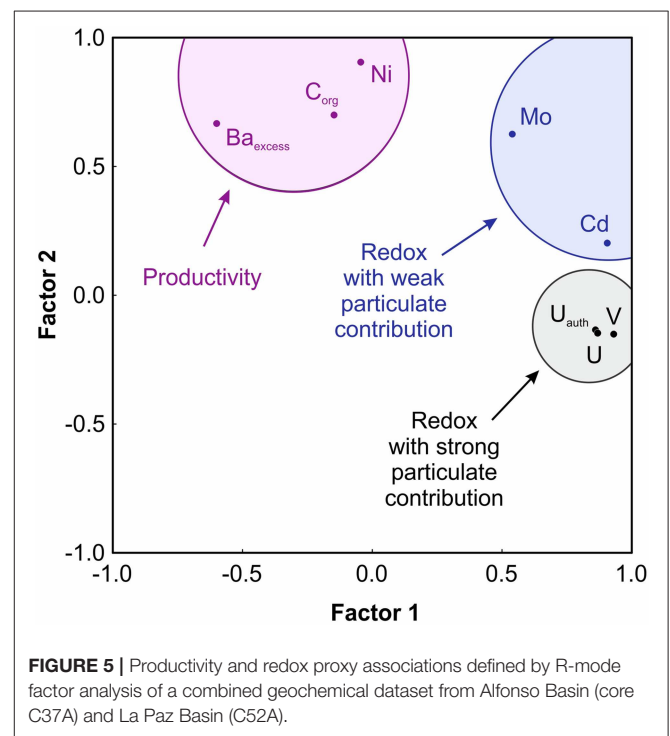
**TABLE 4 |** Factor loadings of the R-mode Factor Analysis with Varimax rotation performed on a combined dataset of cores C37A (Alfonso Basin) and C52A (La Paz Basin).

Proxy	Factor 1	Factor 2
C <sub>org</sub>	-0.1448	0.6978
Ba <sub>excess</sub>	-0.5988	0.6615
Ni	-0.0413	0.9013
U	0.8700	-0.1489
U <sub>auth</sub>	0.8611	-0.1366
V	0.9316	-0.1517
Cd	0.9046	0.1995
Mo	0.5406	0.6226
Explained variance	3.8581	2.2282
Proportion of total variance	48.23%	27.85%

(48.23% variance) and Factor 2 (27.85% variance) (Table 4; Figure 5). The “productivity” association is based on C<sub>org</sub>, Ni and Ba<sub>excess</sub>—elements related to organic matter production at shallow depths. The “redox with weak particulate contribution” defined by Cd and Mo, which require strongly reducing conditions in bottom waters for strong authigenic enrichments. The “redox with strong particulate contribution” links U, U<sub>auth</sub>, and V—elements that can be supplied through particulate fluxes in oxygen-deficient water column depths and/or enriched diagenetically either under anoxic bottom waters or at the sediment-water interface.

### Comparison of Productivity and Redox Proxies in Core Tops Across Varying OMZ Depths and Productivity Regimes in the ETNP

Here we present a compilation of data from core tops from this and previous studies (Table 5; Figure 6 and Supplementary Figure 4). Comparing core tops, most of the cores collected at upper- and mid-OMZ depths have significantly



stronger C<sub>org</sub>, Ba<sub>excess</sub>, Ni, Mo, and V enrichments compared to shallower cores (e.g., core C42A)—with the latter perhaps representing the fluctuating upper OMZ boundary often exposed to high O<sub>2</sub> levels (Table 5). These enrichments correspond to regions where high chlorophyll is reported in the surface waters associated with eastern North Pacific upwelling (Table 5; Figure 6 and Supplementary Figure 4) (Badan-Dangon et al., 1991; Trasviña-Castro et al., 2003). The elevated C<sub>org</sub>, Ba<sub>excess</sub>, and Ni in these high-chlorophyll regions are likely to indicate enhanced primary productivity in the photic zone but could also reflect strong preservation of refractory organics delivered

from land (Calvert et al., 1996; Burdige, 2007; Bianchi et al., 2016) (Table 5). These productive coastal sectors correspond to severe hypoxia/anoxia in which trace element enrichments reach 75.05–149.08 mg/kg for V and 6.75–7.35 mg/kg for Mo in the deepest cores from La Paz and Pescadero basins, respectively (Table 5; Figure 6). Detrital contributions in such settings are relatively minor (Rodríguez-Castañeda, 2008; Choumiline, 2011). These enrichments are favored by oxygen-deficient conditions in the water column and, in the case of Mo, sulfide accumulation in seawater (Calvert and Pedersen, 1993; Zheng et al., 2000; Tribovillard et al., 2006). The studied core tops from the Eastern Pacific OMZ show Mo values sufficiently high to indicate anoxia but are too low to suggest euxinia (presence of H<sub>2</sub>S) (Table 5; Figure 6A). For comparison, only certain places off the Peruvian margin, where water conditions are extremely reducing even for an OMZ, show Mo values as high as 70 mg/kg (McManus et al., 2006). In contrast, at 265 m depth in the upper portion of the OMZ, core C42A displays low V and Mo values of 26.05 and 0.75 mg/kg, respectively, indicating the presence of some oxygen in the overlying waters and that V and Mo are mostly supplied through detrital inputs.

Uranium is the exception. The U<sub>auth</sub> concentrations are high in the shallower and more-oxygenated core (C42A), reaching 13.17 mg/kg—with values similar to those of the deeper, anoxic core tops (C37A and C52A). We hypothesize that the added contribution of uranium is through its uptake in settling particles and associated anoxic microenvironments. Under oxic and weakly oxic conditions, dissolved uranium is present in its +6 form but is reduced to the insoluble +4 form once oxygen declines further (moderate hypoxia) or disappears (anoxia). This authigenic U is preserved as the organic-rich marine aggregates settle through the water column, in the absence of U<sub>auth</sub> reoxidation even in ventilated waters. This exported authigenic uranium is delivered to the sediments—often showing a stronger correlation with C<sub>org</sub> compared to the relationships between the organic matter and V or Mo (Choumiline, 2011). Evidence for authigenic U enrichments in settling particles was reported by Zheng et al. (2002) in marine basins of the California Margin and also from Alfonso Basin, with particulate U concentrations reaching 40 mg/kg (Choumiline et al., 2010; Choumiline, 2011)—more than an order of magnitude higher than the crustal average of 2.5 mg/kg (Wedepohl, 1995).

Like U<sub>auth</sub>, V is enriched in sediments from regions of the Pacific where bottom water anoxia is present. Additionally, its concentration in suspended particles also peaks seasonally at depths of 150–250 m in response to intra-annual changes in water column O<sub>2</sub> (Hakspiel-Segura et al., 2016). The contribution of V to the bottom via settling particles is usually lower than the average sedimentary concentration under low O<sub>2</sub> conditions but still within the same order of magnitude (Rodríguez-Castañeda, 2008).

To assess the contribution of authigenic U through settling, we contrast U and Mo sedimentary records published in the literature with ours from the ETNP (Ivanochko and Pedersen, 2004; McManus et al., 2006). Typically, Mo is used as an indicator for water euxinia (Calvert and Pedersen, 1993; Algeo and Lyons, 2006; Algeo and Tribovillard, 2009; Lyons et al., 2009; Algeo and

Rowe, 2012; Scott and Lyons, 2012), but most of the enrichments in modern OMZs are likely tied to the presence of sulfide only in pore waters (Scholz et al., 2017; Hardisty et al., 2018). We are not using V because, like U, there could also be important contribution of the redox sensitive element through settling particles, associated to reducing microenvironments (Table 5; Choumiline, 2011). We expect good correlation between U and Mo records if both elements are enriched during burial (i.e., diagenetically or at the sediment-water interface; Klinkhammer and Palmer, 1991; Calvert and Pedersen, 1993; Zheng et al., 2002; Algeo and Tribovillard, 2009). A weak correlation is likely to be found for samples where significant amounts of non-lithogenic U are scavenged into particles and settle through the water column. In contrast, Mo uptake is typically limited to the sediments when oxygen is present in the water column. For the previously published data, we estimated bottom O<sub>2</sub> values for each sediment core in a GIS using an interpolated global oxygen database (World Ocean Atlas, 2005; Garcia et al., 2006). This approach allowed us to classify data in two main groups depending on the dominant redox conditions: oxic to moderately hypoxic (0.5 mL/L < [bottom O<sub>2</sub>] < 1.5 mL/L) (Figure 7A) and severely hypoxic (0.1 mL/L < [bottom O<sub>2</sub>] < 0.5 mL/L) to anoxic ([bottom O<sub>2</sub>] < 0.1 mL/L) (Figure 7B). We found that sediments underlying oxic–moderately hypoxic waters do not show correlation between U and Mo—with an R<sup>2</sup> value close to 0.00 (Figure 7A). Some samples do, however, show significant enrichment above crustal values of 2.5 mg/kg that could be due to water column U authigenesis (Zheng et al., 2002; Choumiline, 2011). In contrast, sediments deposited under severely hypoxic to anoxic waters show strong correlation between Mo and U, with an R<sup>2</sup> value of 0.80. While most of the U concentrations for the oxygen-deficient sites correlate with Mo, some reach even higher values of 17 mg/kg U with no significant Mo increase. In many cases, the lack of Mo enrichments could be attributed to bottom water redox potentials that were not sufficiently reducing, especially for sites in the upper OMZ. These observations of high U and low Mo could also indicate a water column supply of authigenic U through settling particles. In this context of U–Mo relationships, the studied sites from Alfonso and La Paz basins fall above the trend line, showing potential surpluses in U<sub>auth</sub> enrichments perhaps tied to high levels of productivity and associated particle scavenging (Figure 7).

## Chronology of Reoxygenation and Deoxygenation Events Over the Past Millennium in a Predominantly Anoxic Marine Setting

In the following discussing, we use the term reoxygenation to imply a relative increase in dissolved O<sub>2</sub> at OMZ depths, usually corresponding to deepening of the upper OMZ boundary. Reoxygenation need not indicate disappearance of the OMZ, as no proxy record indicates fully oxygenated water conditions (Tems et al., 2016), including the data produced in our study—specifically, Mo, V, and U values are several times higher than their crustal average values (Wedepohl, 1995). The oxygenation chronology of the last millennium starts with the predominantly

**TABLE 5** | Comparison of productivity and/or redox proxy values for selected sedimentary material from different OMZ depths in the Eastern Pacific.

Marine basin	Water column depth	Redox condition and bottom dissolved O <sub>2</sub> (mL/L)	Proxy data							
			Productivity/nutrients			Redox and/or Productivity		Redox		
			C <sub>org</sub> (%)	B <sub>a</sub> excess (mg/kg)	Ni (mg/kg)	U (mg/kg)	U <sub>auth</sub> (mg/kg)	Cd (mg/kg)	Mo (mg/kg)	V (mg/kg)
Alfonso Basin, Gulf of California (settling particles) <sup>c</sup>	Upper OMZ (360 m)	Anoxia (<0.1)	7.80 [16.37]	338.95* [2147.45]	37.49 [107.99]	4.65 [42.79]	4.16 [42.70]	1.42 [4.65]	1.40 [7.92]	38.96 [84.64]
Alfonso Basin, Gulf of California (core C42A) <sup>a</sup>	Uppermost OMZ (265 m)	Severe hypoxia (~0.3)	2.96	175.70	26.84	14.31	13.17	5.34	0.75	26.05
Alfonso Basin, Gulf of California (core C37A) <sup>a</sup>	Upper OMZ (408 m)	Anoxia (<0.1)	6.01	406.37	40.25	9.85	8.14	2.48	6.34	124.67
La Paz Basin, Gulf of California (core C52A) <sup>a</sup>	Middle OMZ (785 m)	Anoxia (<0.1)	6.41	682.77	49.06	8.84	7.24	2.60	6.75	75.05
Pescadero Slope, Gulf of California (core DIPAL-III T2) <sup>b</sup>	Upper OMZ (577 m)	Anoxia (<0.1)	6.42	654.95	54.10	8.09	5.05	-	7.35	149.08
Santa Barbara Basin, Eastern Pacific, 34°N (core ODP 893A) <sup>d</sup>	Upper OMZ (576.5 m)	Anoxia (<0.1)	3.00	513.2*	51.00	2.90	-	2.80	4.70	186.70
Mazatlan Margin, Eastern Pacific, 22.7°N (core Mazatlan) <sup>e</sup>	Upper OMZ (442 m)	Anoxia (<0.1)	-	-	-	4.29	-	-	6.26	-
Soledad Basin, Eastern Pacific, 25.2°N (core Soledad) <sup>e</sup>	Upper OMZ (542 m)	Anoxia (<0.1)	7.09	-	-	6.78	-	-	4.16	-
Gulf of Tehuantepec, Eastern Pacific, 15.7°N (core ME0005A 11PC) <sup>f</sup>	Upper OMZ (574 m)	Anoxia (<0.1)	4.74	-	-	-	-	3.05	6.51	-
Gulf of Tehuantepec, Eastern Pacific, 15.7°N (core ME0005A 3JC) <sup>f</sup>	Middle OMZ (740 m)	Anoxia (<0.1)	4.34	-	-	-	-	1.57	6.54	-
Peru Margin Eastern Pacific, 13.7°S (core MC82) <sup>g</sup>	Uppermost OMZ (264 m)	Anoxia (<0.1)	16.27	-	-	17.34	-	-	70.08	-
Upper Continental Crust Average <sup>g</sup>	-	-	-	668*	18.6	2.5	2.5*	0.102	1.4	53

The core top values represent the uppermost 2 cm of sedimentary record.

\*Total concentration value (not enough supplementary data to calculate authigenic or excess values).

<sup>a</sup>This study.

<sup>b</sup>Gravity core (Choumilline et al., 2017).

<sup>c</sup>Sediment trap material; average and [maximum] values between 2002–2008 in 173 samples (Rodríguez-Castañeda, 2008; Choumilline, 2011; Silverberg et al., 2014).

<sup>d</sup>Drill core (Ivanochko and Pedersen, 2004).

<sup>e</sup>Multicore (McManus et al., 2006).

<sup>f</sup>Sediment core (Hendy and Pedersen, 2006).

<sup>g</sup>Wedepohl (1995).

warm climatic trends of the Medieval Warm Period (or Medieval Climate Optimum), which ended as cooling began with gradual change in the insolation regime after the Wolf Minimum (Figure 8). This cooling transitioned the planet into the colder Little Ice Age, which started around 1300 AD (Bard et al., 2000; IPCC, 2014; Griffiths et al., 2016) and was the most anoxic period of the last millennium as indicated by our V, Cd, Mo, and U<sub>auth</sub> data from Alfonso. The Little Ice Age coincides with

the highest values of the SOI index, indicating more La Niña-like years and enhanced upwelling (Yan et al., 2011; Griffiths et al., 2016). Most marine basins of the ETNP experienced short-term reoxygenation events and corresponding decreases in water column denitrification during warm times around late 1300s, early 1700s, and the mid to late 1900s (Figure 8). These warm reoxygenation periods lasted from 100 to 150 years but reversed several times toward anoxic conditions in a matter of decades due

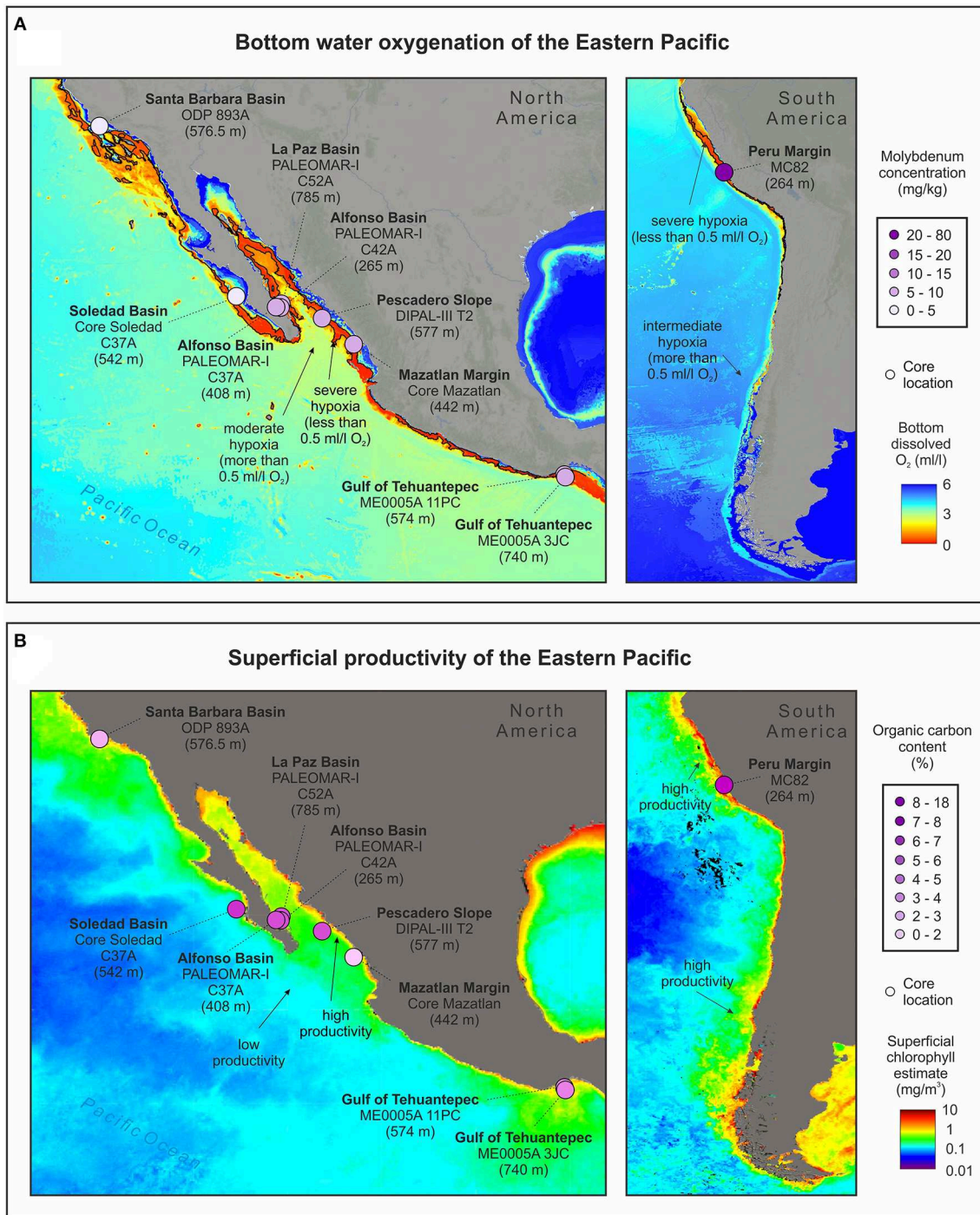
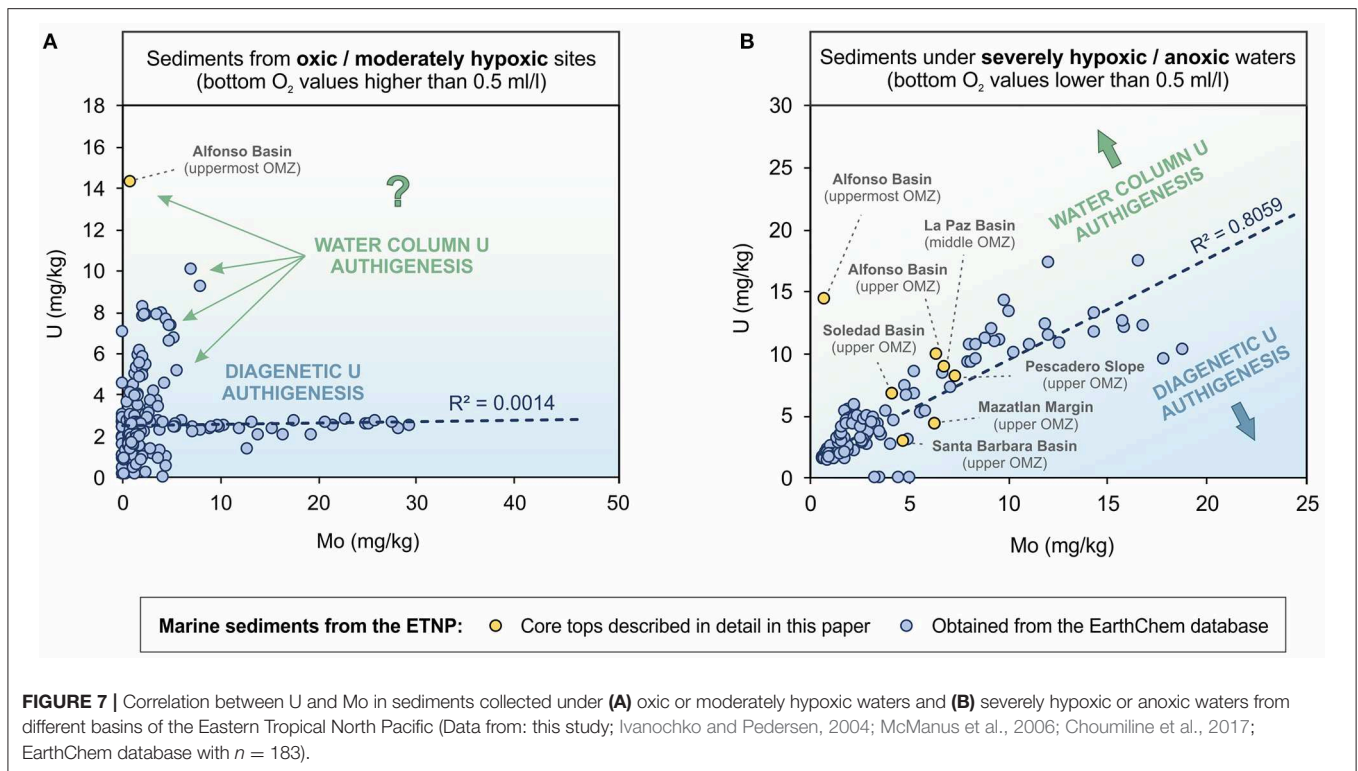


**FIGURE 6 |** Molybdenum and organic carbon in core tops from various locations across the Gulf of California and adjacent Pacific, **(A)** bottom dissolved oxygen, and **(B)** superficial chlorophyll estimate from the studied marine OMZ settings of ETNP (Alfonso Basin and La Paz Basin) (Oxygen based on World Ocean Atlas, 2005; Garcia et al., 2006; superficial chlorophyll estimates by SeaWiFS satellite sensor published by OBPG/NASA).

to cooling and strengthening of the OMZ (Tems et al., 2016). During the Little Ice Age, denitrification, and bottom anoxia were the strongest during the Spörer Minimum, leading to OMZ expansion (this study; Tems et al., 2016). Subsequent periods of

lower solar irradiance (Maunder and Dalton minimums) also corresponded with expanded OMZs but to a lesser degree than during the Spörer (**Figure 8**). The most recent stage was marked by a gradual reoxygenation during the twentieth century toward



the mid-1990s, followed by a slight possible OMZ intensification over the last decade as shown by some of our proxy V and  $U_{\text{auth}}$  data from Alfonso and La Paz basins in accordance with the findings of Tems et al. (2016), Ontiveros-Cuadras et al. (2019) and a high-resolution U record of the last century by Choumiline et al. (2010) and Choumiline (2011).

## Climatic Drivers of Historical OMZ Fluctuations in the ETNP Over the Last Millennium

As suggested by our data from marine basins of the southwestern Gulf of California, patterns of productivity tied to upwelling are one of the key drivers of oxygenation in coastal OMZs. Importantly, most of the variability in the ETNP is indirectly controlled by short and long-term variations of solar irradiance (Bard et al., 2000). La Niña years are known to positively impact productivity in coastal regions of the Eastern Pacific by increasing upwelling rates (Thunell, 1998; Chang et al., 2013). Atmospheric dynamics, also triggered by insolation changes, play a substantial role in controlling coastal wind-driven upwelling, caused by migrations of NPH and ITCZ (Schneider et al., 2014; Metcalfe et al., 2015; Staines-Urías et al., 2015). Southward position of the NPH and ITCZ would trigger more upwelling in the Eastern Pacific (Metcalfe et al., 2015). Our research suggests—based on the chronology of Ni, V, and  $U_{\text{auth}}$  variability—that one of the most important controls on upwelling in the ETNP leading to OMZ fluctuations is the position of the Walker Circulation and its effect on El Niño or La Niña years on longer

time scales (Figure 8). Evidence for long-term ENSO trends are manifested in PDO and/or NPGO variability in the Eastern Tropical North Pacific (Mantua and Hare, 2002; Moy et al., 2002; Di Lorenzo et al., 2010; Choumiline, 2011; Tems et al., 2016). These changes control delivery of nutrients to the marine basins of the Eastern Pacific, subsequently enhancing productivity and favoring oxygen loss (deoxygenation) of these oceanic settings (and OMZs). The mechanistic links between changes in PWC and PDO and their impacts on upwelling variability are still not clear, mainly due to difficulties in the paleoreconstruction of these phenomena.

Our record of productivity and redox over the last millennium can be compared to changes in COCOC (Composite Coccolith Proxy) presented by Beaufort and Grelaud (2017) in an attempt to reconstruct long-term variation in the PDO (Figure 8). The Southern Oscillation Index (SOI) presented by Yan et al. (2011) and Griffiths et al. (2016) is proposed to represent changes in Walker Circulation through time (Figure 8). On decadal and centennial timescales, the driving force for the major and minor fluctuations in the PWC is solar irradiance (Bard et al., 2000). Colder periods corresponding to the solar irradiance minimums—known as Dalton, Maunder, Spörer, and Wolf minimums—are also times of higher productivity and lower oxygen concentrations (seen in the Alfonso, La Paz, and Pescadero records). Importantly, denitrification was also higher during times of low insolation, as evidenced by higher sedimentary  $\delta^{15}\text{N}$  values on the Pescadero Slope (eastern side of the Gulf of California) published by Tems et al. (2016). Periods of high productivity are captured in records for  $\text{Ba}_{\text{excess}}$ ,

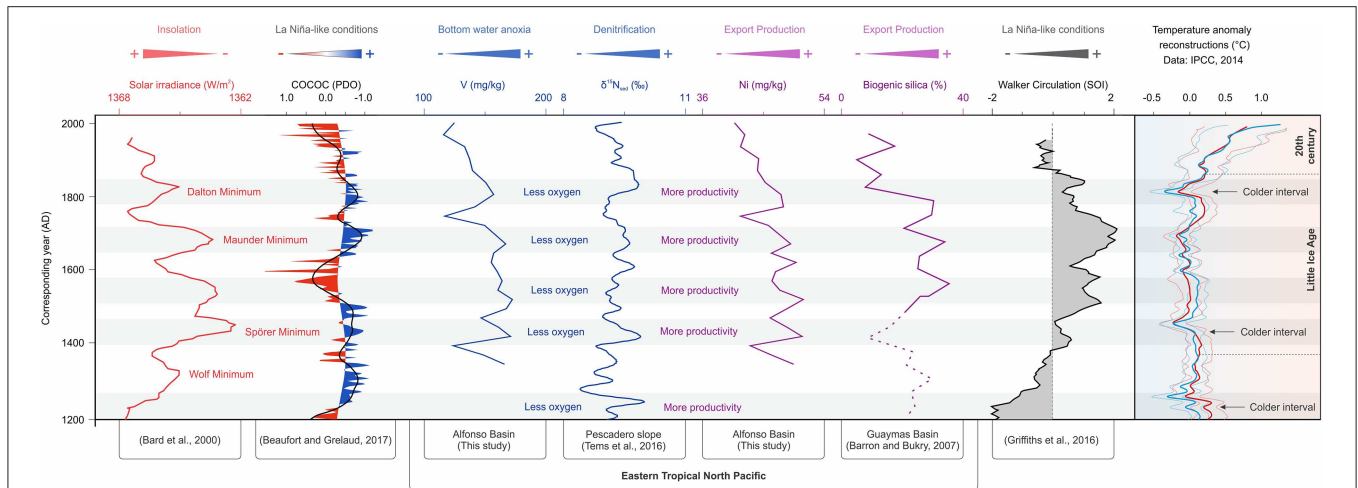


**FIGURE 8 |** Reconstruction of OMZ variability of the Eastern Pacific during the last 800 years based on proxies for water column denitrification, redox and productivity compared to major climatic forcings. Note that the solar irradiance plot is inverted for better visualization.

Ni, and  $U_{\text{auth}}$  in Alfonso and La Paz basins during the Little Ice Age—with maximum peaks of productivity during Spörer, Maunder, and Dalton solar minima (Bard et al., 2000; Barron and Bukry, 2007). Independent records of biogenic silica from Guaymas Basin, central Gulf of California, confirm elevated export production during colder solar episodes (Barron and Bukry, 2007). These productive times led to enhanced bottom water anoxia manifested in high  $V$  and  $U_{\text{auth}}$  concentrations in marine sediments of Alfonso and La Paz basins (Figures 8, 9A). The drivers of climatic change over the last millennium remain unclear, but the leading theories involve a combination of factors from orbital change to periods of strong volcanism that triggered a cooling phase during the Little Ice Age (Atwood et al., 2016). That cooling phase affected the strength of the PWC and led to lesser El Niño years.

### Drivers of Redox in the Eastern Pacific and Apparent Contradictions With the Glacial-Interglacial Model for OMZ Expansions

The mechanisms that control decadal to centennial oxygen variability in the ETNP remain unresolved but are likely influenced by solar forcing. That forcing not only drives migration of the ITCZ (Schneider et al., 2014) but also, more importantly, variation in the intensity of the PWC. During the Little Ice Age, solar irradiance was at its lowest over the past millennium, which strengthened Walker Circulation (Bard et al., 2000; Yan et al., 2011; Griffiths et al., 2016). The result was La Niña-like conditions, which enhanced upwelling of colder nutrient-rich waters and favored elevated productivity and reduced bottom oxygen levels (Figure 9A), as seen in Alfonso and La Paz basins and on the Pescadero Slope (Figure 8). A smaller-scale form of PWC variability is expressed in changes in the PDO and/or NPGO indices, which control rates of denitrification in OMZ waters of the Eastern Pacific (Di Lorenzo et al., 2010; Tems et al., 2016; Beaufort and Grelaud, 2017). As indicated by Tems et al. (2016) and confirmed by our findings,

despite a decline in measured  $O_2$  values in the Eastern Pacific over the last few decades (Bograd et al., 2003, 2008; Levin, 2018), sedimentary records of the ETNP do not indicate increasing anoxia. Our geochemical proxy data from Alfonso from this study, Pescadero (Tems et al., 2016), and Mazatlan Margin (Ontiveros-Cuadras et al., 2019) also confirm that despite the recent warming trend and related anthropogenically triggered ocean-scale  $O_2$  decline (Bograd et al., 2003, 2008; Breitburg et al., 2018; Levin, 2018), the sedimentary records of benthic foraminifera,  $\delta^{15}N$ , Cd, Mo,  $U_{\text{auth}}$ , and  $V$  do not suggest a significant increase in anoxia after the mid-1800s (Figures 4, 8). Our evidence for gradually increasing dissolved oxygen levels are also supported by a decline in export production toward the beginning of the twenty-first century, evidenced by our  $C_{\text{org}}$  and Ni data from Alfonso and La Paz, as well as biogenic silica from Guaymas Basin (Barron and Bukry, 2007).

Despite a longstanding decrease of productivity and redox during the last century (Figure 8), a subtle regime change toward increased anoxia could have begun around the 1990s but is represented only by a few data points for the redox proxies (this study; Dean et al., 2004; IPCC, 2014; Tems et al., 2016). Remarkably, this relationship is only evidenced by  $\delta^{15}N$ ,  $V$ , and Mo and not by productivity proxies, pointing at the global decline of  $O_2$  (Tems et al., 2016; Breitburg et al., 2018; Levin, 2018). Rather than reflecting global warming, reoxygenation and deoxygenation scenarios of the last millennium in the ETNP are primarily controlled by coastal productivity and dominated by long-term persistence of La Niña conditions more often occurring during stronger PWC. Deutsch et al. (2014) proposed another mechanism for the apparent OMZ contraction despite declining  $O_2$  trends in the North Pacific. The authors argued that global warming is resulting in a weakening of easterly trade winds and will continue to do so, leading to contraction of the ETNP OMZ rather than the previously predicted expansion (Deutsch et al., 2014; Tems et al., 2016). Regardless of the dominant mechanisms, our results (Figure 8) also support the

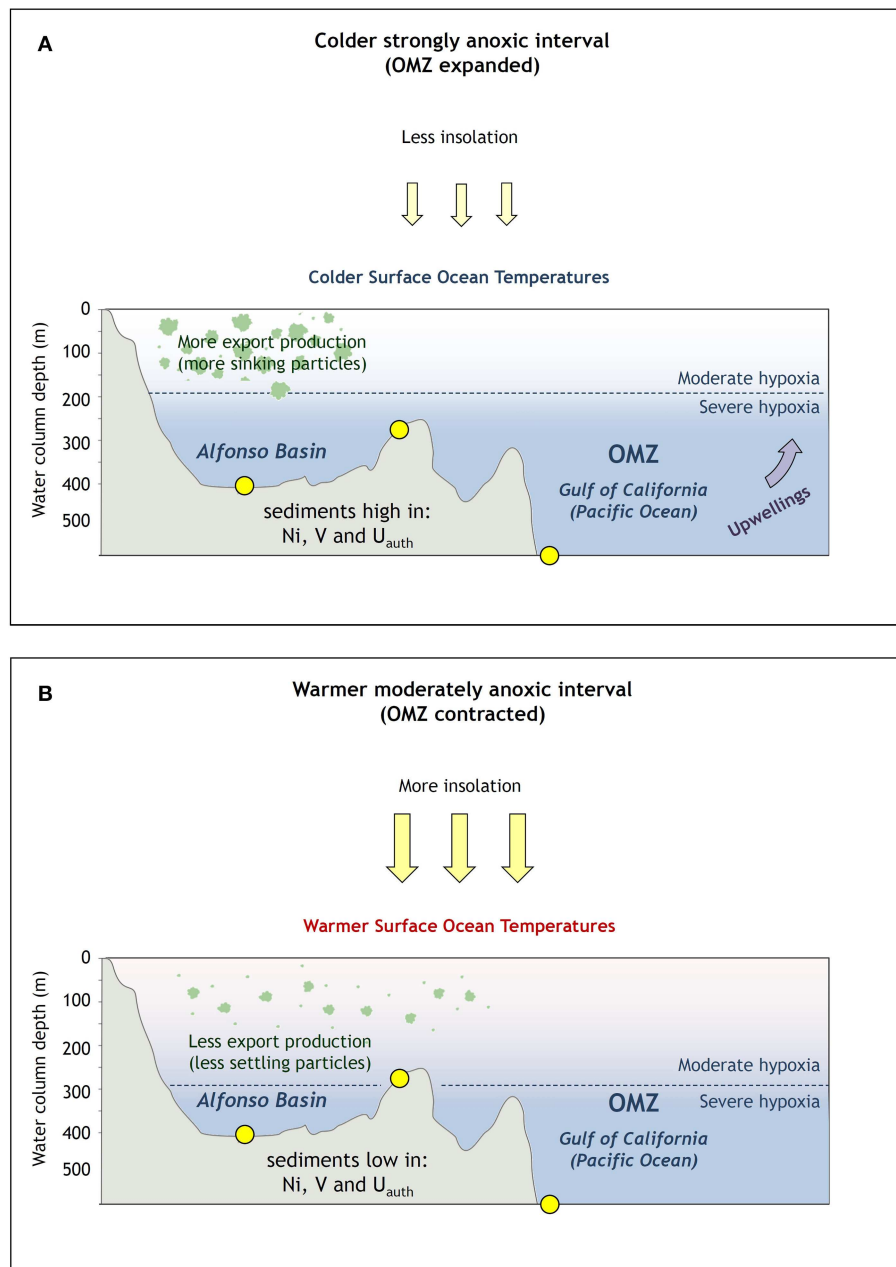


**FIGURE 9** | Two dominating oceanographic regimes: **(A)** high productivity and enhanced anoxia during colder periods, **(B)** low productivity and reoxygenation during warm periods.

interpretation that OMZ expansion occurred during cooling periods rather than being a consequence of warming—at least over the last millennium (**Figure 9**).

A clear distinction should be made between the dominant mechanisms that control oxygenation in the ETNP over decadal-centennial timescales (Deutsch et al., 2014; Tems et al., 2015, 2016) and those that govern long-term glacial-interglacial variability (Ganeshram and Pedersen, 1998; Nameroff et al., 2004; Hendy and Pedersen, 2006; Ivanochko et al., 2008; Pichevin et al., 2012, 2014; Cartapanis et al., 2014; Umling

and Thunell, 2017). High-amplitude variability (such as the one described in our results) is superimposed over the long-term millennial-multimillennial  $O_2$  trends (Nameroff et al., 2004; Cartapanis et al., 2014; Chang et al., 2014; Moffitt et al., 2015; Praetorius et al., 2015; Tetard et al., 2017). In contrast, the long-term tendencies (e.g., transition from the Last Glacial Maximum toward the Holocene) are driven by global changes in temperature and circulation that control intermediate and deep-water oxygenation (Ganeshram and Pedersen, 1998; Hendy and Pedersen, 2006; Cartapanis et al., 2014; Praetorius et al.,

2015; Lu et al., 2016; Choumiline et al., 2017; Breitburg et al., 2018; Levin, 2018). In other words, short-term decreases in anoxia during warm times in response to the weakening of the Walker Circulation and increase abundance of ENSO years can counteract long-term warming of the upper ocean, which causes stratification and reduced ventilation and O<sub>2</sub> concentration on the global scale ocean.

### Lagged Response of the Ocean to Climate Change and Future Scenarios

The effect of global warming on the world ocean is not expected to be spatially uniform. For example, latitudinal differences in the change of O<sub>2</sub> volume have been observed, with faster declines near the equator (0–20°N) compared to higher latitudes (20–90°N) (Schmidtko et al., 2017). Some vulnerable regions have experienced a rapid response (e.g., ETSP), while others (e.g., ETNP) show a lag of several decades (Chavez et al., 2011; Howes et al., 2015; Long et al., 2016). It has been suggested that the response time of the OMZs to ocean deoxygenation caused by a decrease in O<sub>2</sub> solubility and enhanced stratification linked to global warming (Praetorius et al., 2015) could be quicker than 25 years (Tems et al., 2016). However, the effects of climate change on OMZ oxygenation seem to only begin toward the end of the 20th century as preserved in multiple sediment records (Dean et al., 2004; Tems et al., 2016)—including ours—wherein the gradual oxygen increase in the beginning of the twentieth century shifts to a decline in O<sub>2</sub> toward the twenty-first century. The observed lagged response in O<sub>2</sub> trends to warming is consistent with current estimates of oceanic oxygen volume (Chavez et al., 2011; Long et al., 2016; Schmidtko et al., 2017).

Overall, there is still no consensus in the community about predicted OMZ behavior for the near future due to differences in the volume estimates among the models (Cocco et al., 2013; Long et al., 2016; Battaglia and Joos, 2018). A more recent study concludes that after the gradual increase of anoxia, the trend will be reversed globally, and the overall volume of OMZs will start declining (Fu et al., 2018). The mechanism proposed by Fu et al. (2018) involves a reduction of biological export linked to surface warming.

## SYNTHESIS

### Lessons Learned About the Utility of Productivity and Redox Proxies From Our ETNP OMZ Records

Our findings indicate that the efficacy of productivity and redox proxies in modern OMZs depends somewhat on the supply of non-detrital trace elements via settling due to biological uptake or scavenging, as well as their preservation potential during diagenetic overprinting. We conclude that Ni, U, and V are the most reliable, while Ba and Mo should be used with caution in OMZ-type settings. Barium is significantly enriched in sediment trap material, which could elevate its proxy potential in the region (Table 5; Rodríguez-Castañeda, 2008; Choumiline, 2011). However, its long-term preservation in sedimentary records is an important issue. For La Paz Basin, we

can confirm that Ba<sub>excess</sub> did not behave as a reliable productivity proxy—showing trends that differ significantly from those of the other indicators (Table 3). However, our Ba<sub>excess</sub> record in Alfonso Basin does mirror other productivity proxies (C<sub>org</sub> and Ni) and is statistically associated with them (Figure 5). This agreement could be because our Alfonso Basin core was not exposed to severe diagenetic remobilization of sedimentary barite as much as the La Paz basin core (McManus et al., 1998; Riedinger et al., 2006). Despite the good agreement between proxy records and Ba<sub>excess</sub> in Alfonso Basin, long-term preservation of the Ba fraction remains a concern (Schoepfer et al., 2015).

In our studied cores, Ni shows good temporal agreement with both the productivity (C<sub>org</sub> and Ba<sub>excess</sub>) and water column redox proxies (V and U<sub>auth</sub>). In Alfonso Basin, this element served as the best indicator for productivity—mirroring an independent biogenic SiO<sub>2</sub> record from Guaymas Basin generated by Barron and Bukry (2007) (Figure 8). Nickel does not follow Mo and Cd, which are bottom water and/or diagenetic redox proxies (Figure 5), which could be explained by a significant contribution of particulate Ni (Table 5), enriched in settling matter by biological uptake (Böning et al., 2015) and potentially related to diatom export (Twining et al., 2012).

In our sediment cores from Alfonso and La Paz basins, Mo covaries with Cd (Figure 5) and reaches high values. However, due to the low and transient concentrations of water column H<sub>2</sub>S in most modern OMZs, it is unlikely that Mo enrichments are related to bottom water euxinia in such settings (Scott and Lyons, 2012; McKay and Pedersen, 2014; Costa et al., 2018). Nevertheless, Mo is commonly elevated in ETNP sediment cores, reaching maxima several times higher than the average crustal value of 1.4 mg/kg (Wedepohl, 1995) (Figure 7; Table 5). These values are likely linked to the presence of sulfide only in the pore waters, leading to diagenetic enrichments (Zheng et al., 2000; Scholz et al., 2017; Hardisty et al., 2018). Because of this diagenetic enrichment, Mo is a less sensitive indicator of very low and transient sulfide in the water column.

We confirm the utility of V as a water column redox proxy as expressed through strong correlation with water column denitrification records reconstructed from sedimentary δ<sup>15</sup>N in the ETNP OMZ (Tems et al., 2016). Moreover, V is sensitive to O<sub>2</sub> changes occurring not only at upper OMZ depths but also those closer to the OMZ-core, which have less pronounced redox variations. It is worth noting that, as for U<sub>auth</sub>, there is evidence for an important contribution of V through settling matter (Rodríguez-Castañeda, 2008; Hakspiel-Segura et al., 2016; Bauer et al., 2017; Ho et al., 2018). The source of such enrichments is yet unknown, but we hypothesize that it could be related to redox processes causing authigenic V enrichment in organic matter aggregates (Ho et al., 2018).

An important methodological distinction needs to be made for proper numerical treatment of sediments with highly variable CaCO<sub>3</sub> and biogenic silica contents. As previously suggested (Pichevin et al., 2012, 2014), proxy records can, in some cases, be significantly impacted by dilution with major components. In this study we have CaCO<sub>3</sub> values for the studied sediment cores, so CFB fraction calculations were possible. By comparing elemental

concentrations against CFB-corrected values, no substantial differences were found. Most importantly, the paleoceanographic and paleoclimatic trends described in this paper also prevailed for the carbonate-corrected values. We have no data to corroborate the dilution effect with biogenic opal, as it was not measured for the cores studied here. The consequences of the dilution effects with biogenic detritus need to be further investigated for Alfonso Basin and similar marine settings.

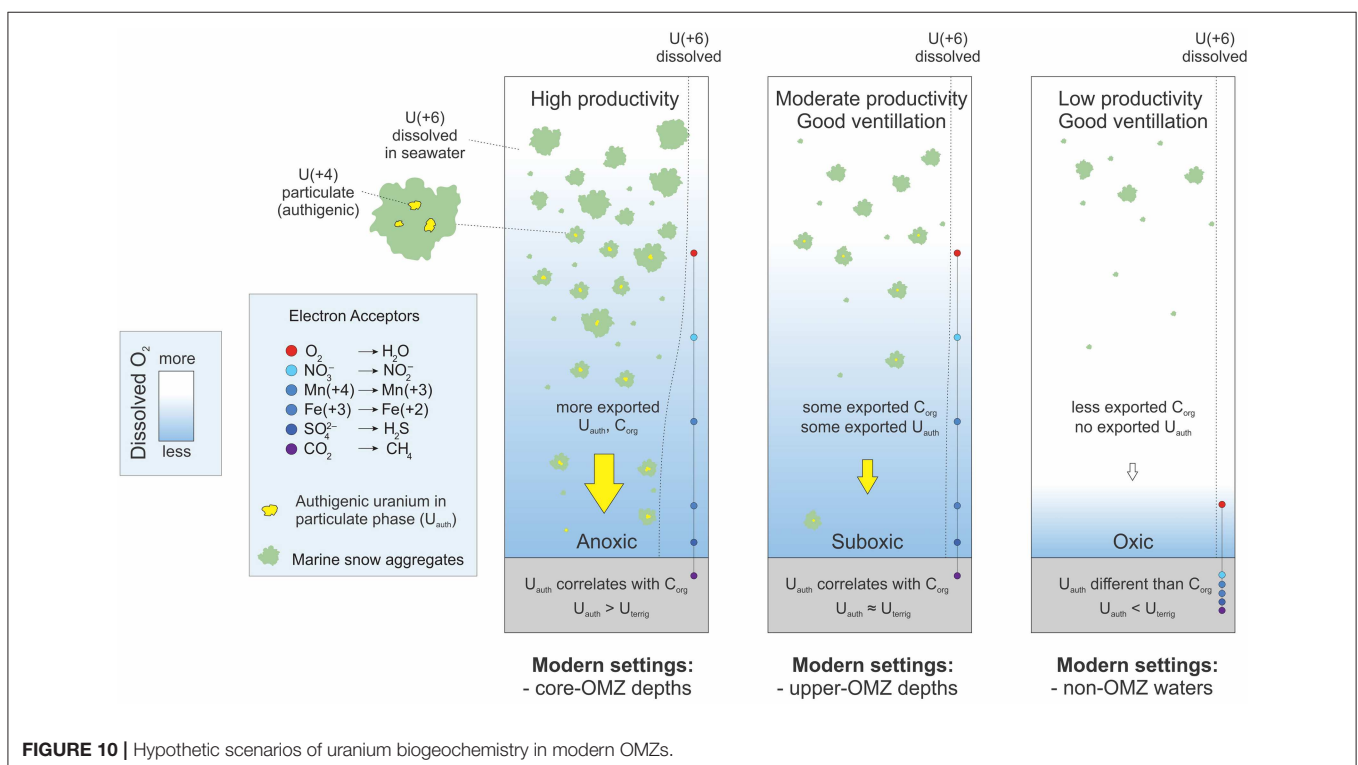
### New Insights on Uranium Biogeochemistry in OMZs

In our study, uranium shows a consistently good correlation with  $C_{org}$  and the micronutrient Ni in both the deeper (mid OMZ) and shallow cores (upper OMZ) (**Figure 4** and **Supplementary Figure 3**). We attribute this observation to seasonal variation in dissolved  $O_2$  and to the particulate authigenic U contribution during settling (Rodríguez-Castañeda, 2008; Choumiline, 2011). As particles settle deeper, there is more reaction time for dissolved U (+6) to be reduced to its particulate phase U (+4) and/or for adsorption to occur. This relationship is a consistent feature of vertical sediment trap moorings—that is, higher authigenic U enrichment in the particles collected in deeper waters (Zheng et al., 2002; Rodríguez-Castañeda, 2008; Huang and Conte, 2009; Choumiline, 2011). The extent to which  $U_{auth}$  enrichments are microbially mediated remains unknown, but evidence suggests that these biological interactions could be among the principal controls (Lovley et al., 1991; Cumberland et al., 2016). There is growing evidence that anaerobic metabolism can occur within aggregates of settling matter if conditions are energetically favorable (Wright et al., 2012; Lehto et al., 2014; Bianchi et al., 2018). Authigenic U

formation is favored after the ferruginous (Fe reduction) and sulfidic ( $SO_4^{2-}$  reduction) chemical zones (Zheng et al., 2002; Canfield and Thamdrup, 2009). This range of redox conditions is common in marine aggregates of modern OMZs (Bianchi et al., 2018), which could explain the strong authigenic U enrichments in settling matter of the Gulf of California and California Margin (Zheng et al., 2002; Choumiline, 2011). Other marine settings, such as Saanich Inlet, also reveal the possibility of water column authigenic U enrichments, where up to one third of the estimated authigenic fraction is captured in particles in the water column (Holmden et al., 2015). It is worth mentioning that while ideal microenvironments for particulate- $U_{auth}$  formation exist in strongly reducing and restricted settings in the Black and Baltic seas, as well as the Cariaco Basin (Dellwig et al., 2010; Calvert et al., 2015; Bauer et al., 2017), significant  $U_{auth}$  enrichments have not been detected (Anderson et al., 1989; Calvert et al., 2015). Perhaps the necessary conditions for authigenic U enrichments are favored in coastal upwelling sites, where high productivity and thus abundant particulate organic matter formation are common.

We propose an updated model for  $U_{auth}$  enrichments (**Figure 10**). This model points to a significant contribution of  $U_{auth}$ , beyond that linked to diagenesis, via settling matter in regions of high productivity and upwelling—such as the coastal regions of the ETNP.

In summary, the current understanding of U geochemistry in OMZs supports a significant contribution via settling particulates during times of high productivity. The actual enrichment mechanism could either be linked to localized reduction within organic-rich microenvironments or simply adsorption to organic



matter. Both processes could explain the correlation with  $C_{org}$  and Ni and excessive U enrichments during well-ventilated times. Improved understanding of the details of U uptake will enhance its utility as a paleoproxy.

## Suggestions for Future Work

This research highlights the importance of comparing high-resolution OMZ records of both modern and past oceanic conditions with global climatic trends. We have demonstrated it is possible to reconstruct high-resolution OMZ variability using a multiproxy approach. However, there are multiple caveats when interpreting deoxygenation and productivity trends because of the complex mechanisms by which trace elements are transferred to sedimentary records. We encourage particular caution for elements that demand an understanding of the relative contributions from diagenetic vs. water column processes and how specifically those inputs translate to regional patterns of redox and productivity. The importance of particulate supply of scavenged non-detrital trace elements in OMZ-type settings is clear, and further research, when possible, should include isotopic data as a source of additional mechanistic perspective.

## CONCLUSIONS

In the modern Eastern Tropical North Pacific, marine sediments are mostly enriched in Cd, Mo, V at sites underlying severely hypoxic and anoxic waters—in contrast to shallower and oxygenated sites where these elements are present in low, mostly crustal, abundances. The exception is U, which is found to be enriched not only in sediments underlying anoxic waters but also in those of well-ventilated regions, suggesting a strong contribution of authigenic uranium through settling of marine snow aggregates.

Most of the sites located at present Oxygen Minimum Zone depths remained anoxic over the last millennium. The Eastern Tropical North Pacific Oxygen Minimum Zone expanded throughout the Little Ice Age, with the most anoxic events during the Spörer, Maunder, and Dalton insolation minima. Reoxygenation in the Eastern Tropical North Pacific occurred during warm periods around late 1300s, early 1700s, and late 1900s AD.

There is no clear effect of the temperature increase of twentieth century on the intensification of the Eastern Tropical North Pacific Oxygen Minimum Zone. The prevailing trend shows an increase in dissolved oxygen from the 1900s AD toward present time, with a subtle decrease in the beginning of the twenty-first century.

## REFERENCES

- Algeo, T. J., and Lyons, T. W. (2006). Mo-total organic carbon covariation in modern anoxic marine environments: implications for analysis of paleoredox and paleohydrographic conditions. *Paleoceanogr. Paleoclimatol.* 21:PA1016 doi: 10.1029/2004PA001112
- Algeo, T. J., and Rowe, H. (2012). Paleoceanographic applications of trace-metal concentration data. *Chem. Geol.* 324–325, 6–18. doi: 10.1016/j.chemgeo.2011.09.002

Redox and productivity changes reconstructed for the last millennium from marine basins of the Eastern Tropical North Pacific indicate a strong relationship with insolation fluctuations and the Pacific Walker Circulation that drive upwelling rates, productivity, and oceanic anoxia at Oxygen Minimum Zone depths.

The most reliable redox proxies for water column oxygenation in Oxygen Minimum Zones are vanadium and uranium. Uranium also shows strong potential to serve as a productivity proxy because it can be exported from the water column to sediments through settling particulate matter during periods of high primary productivity. Molybdenum is the least useful proxy for Oxygen Minimum Zone oxygenation because it is not sensitive to small redox variations and can be enriched diagenetically when pore water sulfide is present.

## AUTHOR CONTRIBUTIONS

KC wrote the paper including comments by LP-C, AG, SB, and TL. Project planning logistics were performed by KC, TL, and LP-C. Samples used in this research were collected, preserved, and handled by KC and LP-C. Analytical measurements were performed by KC, SB, and AG.

## ACKNOWLEDGMENTS

The authors acknowledge financial support granted by UC MEXUS - CONACYT Collaborative Research Grant “High resolution geochemical reconstructions of recent climate and oxygenation history in La Paz Bay, Gulf of California” that covered travel and analytical costs. The authors express gratitude to Coordinación de Plataformas Oceanográficas (UNAM, Mexico) for funding the PALEOMAR-I campaign and the crew members of R/V “El Puma” for exceptional support during the field stage. KC was thankful for the UC MEXUS – CONACYT Doctoral Fellowship for a fully funded scholarship during his Ph.D. studies and for the 2016 UC MEXUS Dissertation Grant award for analytical expenses. Partial support was received by TL, KC, and SB from the NASA Astrobiology Institute, and AG from the USDA NIFA Hatch program (project # CA-R-ENS-5120-H).

## SUPPLEMENTARY MATERIAL

The Supplementary Material for this article can be found online at: <https://www.frontiersin.org/articles/10.3389/feart.2019.00237/full#supplementary-material>

- Algeo, T. J., and Tribouillard, N. (2009). Environmental analysis of paleoceanographic systems based on molybdenum–uranium covariation. *Chem. Geol.* 268, 211–225. doi: 10.1016/j.chemgeo.2009.09.001
- Anderson, R. F., Fleisher, M. Q., and Leheray, A. P. (1989). Concentration, oxidation state, and particulate flux of uranium in the Black Sea. *Geochim. Cosmochim. Acta* 53, 2215–2224. doi: 10.1016/0016-7037(89)90345-1
- Anderson, R. F., and Winckler, G. (2005). Problems with paleoproductivity proxies. *Paleoceanogr. Paleoclimatol.* 20:PA3012. doi: 10.1029/2004PA001107

- Atwood, A. R., Wu, E., Frierson, D. M. W., Battisti, D. S., and Sachs, J. P. (2016). Quantifying climate forcings and feedbacks over the Last Millennium in the CMIP5-PMIP3 Models. *J. Clim.* 29, 1161–1178. doi: 10.1175/JCLI-D-15-0063.1
- Badan-Dangon, A., Dorman, C. E., Merrifield, M. A., and Winant, C. D. (1991). The lower atmosphere over the Gulf of California. *J. Geophys. Res.* 96, 16887–16896. doi: 10.1029/91JC01433
- Bard, E., Raisbeck, G., Yiou, F., and Jouzel, J. (2000). Solar irradiance during the last 1200 years based on cosmogenic nuclides. *Tellus B* 52, 985–992. doi: 10.3402/tellusb.v52i3.17080
- Barron, J. A., and Bukry, D. (2007). Solar forcing of Gulf of California climate during the past 2000 yr suggested by diatoms and silicoflagellates. *Mar. Micropaleontol.* 62, 115–139. doi: 10.1016/j.marmicro.2006.08.003
- Battaglia, G., and Joos, F. (2018). Hazards of decreasing marine oxygen: the near-term and millennial-scale benefits of meeting the Paris climate targets. *Earth Syst. Dyn.* 9, 797–816. doi: 10.5194/esd-9-797-2018
- Bauer, S., Blomqvist, S., and Ingri, J. (2017). Distribution of dissolved and suspended particulate molybdenum, vanadium, and tungsten in the Baltic Sea. *Mar. Chem.* 196, 135–147. doi: 10.1016/j.marchem.2017.08.010
- Beaufort, L., and Grelaud, M. (2017). A 2700-year record of ENSO and PDO variability from the Californian margin based on coccolithophore assemblages and calcification. *Prog. Earth Planet. Sci.* 4:5. doi: 10.1186/s40645-017-0123-z
- Bianchi, D., Weber, T. S., Kiko, R., and Deutsch, C. (2018). Global niche of marine anaerobic metabolisms expanded by particle microenvironments. *Nat. Geosci.* 11, 263–268. doi: 10.1038/s41561-018-0081-0
- Bianchi, T. S., Schreiner, K. M., Smith, R. W., Burdige, D. J., Woodard, S., and Conley, D. J. (2016). Redox effects on organic matter storage in coastal sediments during the holocene: a biomarker/proxy perspective. *Annu. Rev. Earth Planet. Sci.* 44, 295–319. doi: 10.1146/annurev-earth-060614-105417
- Bograd, S. J., Castro, C. G., Di Lorenzo, E., Palacios, D. M., Bailey, H., Gilly, W., et al. (2008). Oxygen declines and the shoaling of the hypoxic boundary in the California Current. *Geophys. Res. Lett.* 35:L12607. doi: 10.1029/2008GL034185
- Bograd, S. J., Checkley, D. A., and Wooster, W. S. (2003). CalCOFI: a half century of physical, chemical, and biological research in the California Current System. *Deep Sea Res. Part II Top. Stud. Oceanogr.* 50, 2349–2353. doi: 10.1016/S0967-0645(03)00122-X
- Böning, P., Shaw, T., Pahnke, K., and Brumsack, H.-J. (2015). Nickel as indicator of fresh organic matter in upwelling sediments. *Geochim. Cosmochim. Acta* 162, 99–108. doi: 10.1016/j.gca.2015.04.027
- Borreggine, M., Myhre, S. E., Mislan, K. A. S., Deutsch, C., and Davis, C. V. (2017). A database of paleoceanographic sediment cores from the North Pacific, 1951–2016. *Earth Syst. Sci. Data* 9, 739–749. doi: 10.5194/essd-9-739-2017
- Breitburg, D., Levin, L. A., Oschlies, A., Grégoire, M., Chavez, F. P., Conley, D. J., et al. (2018). Declining oxygen in the global ocean and coastal waters. *Science* 359:eaam7240. doi: 10.1126/science.aam7240
- Brumsack, H.-J., and Gieskes, J. (1983). Interstitial water trace-metal chemistry of laminated sediments from the Gulf of California, Mexico. *Mar. Chem.* 14, 89–106. doi: 10.1016/0304-4203(83)90072-5
- Burdige, D. J. (2007). Preservation of organic matter in marine sediments: controls, mechanisms, and an imbalance in sediment organic carbon budgets? *Chem. Rev.* 107, 467–485. doi: 10.1021/cr050347q
- Bustos-Serrano, H., and Castro-Valdez, R. (2006). Flux of nutrients in the Gulf of California: geostrophic approach. *Mar. Chem.* 99, 210–219. doi: 10.1016/j.marchem.2005.09.012
- Calvert, S. E., Bustin, R. M., and Ingall, E. D. (1996). Influence of water column anoxia and sediment supply on the burial and preservation of organic carbon in marine shales. *Geochimica Cosmochimica Acta* 60, 1577–1593.
- Calvert, S. E., and Pedersen, T. (1993). Geochemistry of recent oxic and anoxic marine sediments: implications for the geological record. *Mar. Geol.* 113, 67–88. doi: 10.1016/0025-3227(93)90150-T
- Calvert, S. E., Piper, D. Z., Thunell, R. C., and Astor, Y. (2015). Elemental settling and burial fluxes in the Cariaco Basin. *Mar. Chem.* 177, 607–629. doi: 10.1016/j.marchem.2015.10.001
- Canfield, D. E., and Thamdrup, B. (2009). Towards a consistent classification scheme for geochemical environments, or, why we wish the term 'suboxic' would go away. *Geobiology* 7, 385–392. doi: 10.1111/j.1472-4669.2009.00214.x
- Carpenter, J. H. (1965). The Chesapeake Bay Institute technique for the Winkler dissolved oxygen method. *Limnol. Oceanogr.* 10, 141–143. doi: 10.4319/lo.1965.10.1.0141
- Cartapanis, O., Tachikawa, K., Romero, O. E., and Bard, E. (2014). Persistent millennial-scale link between Greenland climate and northern Pacific Oxygen Minimum Zone under interglacial conditions. *Clim. Past* 10, 405–418. doi: 10.5194/cp-10-405-2014
- Chang, A. S., Bertram, M. A., Ivanochko, T., Calvert, S. E., Dallimore, A., and Thomson, R. E. (2013). Annual record of particle fluxes, geochemistry and diatoms in Effingham Inlet, British Columbia, Canada, and the impact of the 1999 La Niña event. *Mar. Geol.* 337, 20–34. doi: 10.1016/j.margeo.2013.01.003
- Chang, A. S., Pedersen, T. F., and Hendy, I. L. (2014). Effects of productivity, glaciation, and ventilation on late Quaternary sedimentary redox and trace element accumulation on the Vancouver Island margin, western Canada. *Paleoceanography* 29, 730–746. doi: 10.1002/2013PA002581
- Chappaz, A., Lyons, T. W., Gregory, D. D., Reinhard, C. T., Gill, B. C., Li, C., et al. (2014). Does pyrite act as an important host for molybdenum in modern and ancient euxinic sediments? *Geochim. Cosmochim. Acta* 126, 112–122. doi: 10.1016/j.gca.2013.10.028
- Chavez, F. P., Messié, M., and Pennington, J. T. (2011). Marine primary production in relation to climate variability and change. *Ann. Rev. Mar. Sci.* 3, 227–260. doi: 10.1146/annurev.marine.010908.163917
- Choumiline, K. (2011). *Geoquímica de la materia particulada en hundimiento y de los sedimentos recientes de Cuenca Alfonso, Bahía de La Paz*. (Master's thesis). Centro Interdisciplinario de Ciencias Marinas – Instituto Politécnico Nacional, La Paz, Mexico.
- Choumiline, K., Lyons, T. W., Pérez-Cruz, L., Carriquiry, J. D., Raiswell, R., and Beaufort, L. (2017). "Sensitivity of redox proxies to rapid variability in Oxygen Minimum Zones. Goldschmidt 2017," in *Abstract Retrieved from Goldschmidt Conference Archive* (Paris).
- Choumiline, K., Rodríguez-Castañeda, A. P., Silverberg, N., Shumilin, E., Aguirre-Bahena, F., Sapozhnikov, D., et al. (2010). "Arsenic and uranium in the settling particulate matter and sediments of Alfonso Basin, La Paz Bay," in *Proceedings of the 13th International Conference on Water-Rock Interaction. Reviewed Extended Abstract* (Guanajuato).
- Cocco, V., Joos, F., Steinacher, M., Frölicher, T. L., Bopp, L., Dunne, J., et al. (2013). Oxygen and indicators of stress for marine life in multi-model global warming projections. *Biogeosciences* 10, 1849–1868. doi: 10.5194/bg-10-1849-2013
- Conte, M. H., Carter, A. M., Kowek, D. A., Huang, S., and Weber, J. C. (2019). The elemental composition of the deep particle flux in the Sargasso Sea. *Chem. Geol.* 511, 279–313. doi: 10.1016/j.chemgeo.2018.11.001
- Coria-Monter, E., Monreal-Gómez, M. A., Salas-de-León, D. A., Aldeco-Ramírez, J., and Merino-Ibarra, M. (2014). Differential distribution of diatoms and dinoflagellates in a cyclonic eddy confined in the Bay of La Paz, Gulf of California. *J. Geophys. Res.* 119, 6258–6268. doi: 10.1002/2014JC009916
- Costa, K. M., Anderson, R. F., McManus, J. F., Winckler, G., Middleton, J. L., and Langmuir, C. H. (2018). Trace element (Mn, Zn, Ni, V) and authigenic uranium (aU) geochemistry reveal sedimentary redox history on the Juan de Fuca Ridge, North Pacific Ocean. *Geochim. Cosmochim. Acta* 236, 79–98. doi: 10.1016/j.gca.2018.02.016
- Cumberland, S. A., Douglas, G., Grice, K., and Moreau, J. W. (2016). Uranium mobility in organic matter-rich sediments: a review of geological and geochemical processes. *Earth Sci. Rev.* 159, 160–185. doi: 10.1016/j.earscirev.2016.05.010
- Dean, W., Pride, C., and Thunell, R. (2004). Geochemical cycles in sediments deposited on the slopes of the Guaymas and Carmen Basins of the Gulf of California over the last 180 years. *Quat. Sci. Rev.* 23, 1817–1833. doi: 10.1016/j.quascirev.2004.03.010
- Dean, W. E. (2007). Sediment geochemical records of productivity and oxygen depletion along the margin of western North America during the past 60,000 years: teleconnections with Greenland Ice and the Cariaco Basin. *Quat. Sci. Rev.* 26, 98–114. doi: 10.1016/j.quascirev.2006.08.006
- Dellwig, O., Leipe, T., März, C., Glockzin, M., Pollehne, F., Schmetger, B., et al. (2010). A new particulate Mn–Fe–P-shuttle at the redoxcline of anoxic basins. *Geochim. Cosmochim. Acta* 74, 7100–7115. doi: 10.1016/j.gca.2010.09.017
- Deutsch, C., Berelson, W., Thunell, R., Weber, T., Tems, C., McManus, J., et al. (2014). Oceanography. *Centennial changes in North Pacific anoxia linked to tropical trade winds*. *Science* 345, 665–668. doi: 10.1126/science.1252332
- Di Lorenzo, E., Cobb, K. M., Furtado, J. C., Schneider, N., Anderson, B. T., Bracco, A., et al. (2010). Central Pacific El Niño and decadal climate change in the North Pacific Ocean. *Nat. Geosci.* 3, 762–765. doi: 10.1038/ngeo984

- Di Lorenzo, E., Schneider, N., Cobb, K. M., Franks, P. J. S., Chhak, K., Miller, A. J., et al. (2008). North Pacific Gyre Oscillation links ocean climate and ecosystem change. *Geophys. Res. Lett.* 35:L08607. doi: 10.1029/2007GL032838
- Dickens, G. R., Koelling, M., Smith, D. C., and Schnieders, L. (2007). Rhizon sampling of pore waters on scientific drilling expeditions: an example from the IODP Expedition 302, Arctic Coring Expedition (ACEX). *Sci. Drilling* 4, 22–25. doi: 10.5194/sd-4-22-2007
- Dunk, R. M., Mills, R. A., and Jenkins, W. J. (2002). A reevaluation of the oceanic uranium budget for the Holocene. *Chem. Geol.* 190, 45–67. doi: 10.1016/S0009-2541(02)00110-9
- Dupont, C. L., Buck, K. N., Palenik, B., and Barbeau, K. (2010). Nickel utilization in phytoplankton assemblages from contrasting oceanic regimes. *Deep Sea Res. Part I Oceanogr. Res. Pap.* 57, 553–566. doi: 10.1016/j.dsr.2009.12.014
- Durand, A., Chase, Z., Townsend, A. T., Noble, T., Panietz, E., and Goemann, K. (2016). Improved methodology for the microwave digestion of carbonate-rich environmental samples. *Int. J. Environ. Anal. Chem.* 96, 119–136. doi: 10.1080/03067319.2015.1137904
- Durazo-Arvizu, R., and Gaxiola-Castro, G. (2010). *Dinámica del ecosistema pelágico frente a Baja California, 1997–2007. Diez años de investigaciones mexicanas de la Corriente de California.* Mexico, Distrito Federal: INE/CICESE/UABC/SEMARNAT.
- Dymond, J., Suess, E., and Lyle, M. (1992). Barium in deep-sea sediment. A geochemical proxy for paleoproductivity. *Paleoceanography Paleoclimatol.* 7, 163–181. doi: 10.1029/92PA00181
- Eagle, M., Paytan, A., Arrigo, K. R., van Dijken, G., and Murray, R. W. (2003). A comparison between excess barium and barite as indicators of carbon export. *Paleoceanogr. Paleoclimatol.* 18:1021. doi: 10.1029/2002PA000793
- Erickson, B. E., and Helz, G. R. (2000). Molybdenum(VI) speciation in sulfidic waters: Stability and lability of thiomolybdates. *Geochim. Cosmochim. Acta* 64, 1149–1158. doi: 10.1016/S0016-7037(99)00423-8
- Foster, I. D. L., and Walling, D. E. (1994). Using reservoir deposits to reconstruct changing sediment yields and sources in the catchment of the Old Mill Reservoir, South Devon, UK, over the past 50 years. *Hydrol. Sci. J.* 39, 347–368. doi: 10.1080/02626669409492755
- Fu, W., Primeau, F., Moore, J. K., Lindsay, K., and Randerson, J. T. (2018). Reversal of increasing tropical ocean hypoxia trends with sustained climate warming. *Global Biogeochem. Cycles* 32, 551–564. doi: 10.1002/2017GB005788
- Ganeshram, R. S., and Pedersen, T. F. (1998). Glacial-interglacial variability in upwelling and bioproductivity off NW Mexico: implications for quaternary paleoclimate. *Paleoceanography Paleoclimatol.* 13, 634–645. doi: 10.1029/98PA02508
- Garcia, H. E., Locarnini, R. A., Boyer, T. P., and Antonov, J. I. (2006). World Ocean Atlas 2005, Volume 3: Dissolved Oxygen, Apparent Oxygen Utilization, and Oxygen Saturation. S. Levitus, Ed. NOAA Atlas NESDIS 63, U.S. Government Printing Office, Washington, D.C., 342 pp.
- Gilly, W. F., Beman, J. M., Litvin, S. Y., and Robison, B. H. (2013). Oceanographic and biological effects of shoaling of the oxygen minimum zone. *Ann. Rev. Mar. Sci.* 5, 393–420. doi: 10.1146/annurev-marine-120710-100849
- Griffiths, M. L., Kimbrough, A. K., Gagan, M. K., Drysdale, R. N., Cole, J. E., Johnson, K. R., et al. (2016). Western Pacific hydroclimate linked to global climate variability over the past two millennia. *Nat. Commun.* 7:11719. doi: 10.1038/ncomms11719
- Hakspiel-Segura, C., Martínez-López, A., Pinedo-González, P., Verdugo-Díaz, G., and Acevedo-Acosta, J. D. (2016). Composition of metals in suspended particulate matter of Alfonso basin, southern Gulf of California. *Reg. Stud. Mar. Sci.* 3, 144–153. doi: 10.1016/j.rsm.2015.07.001
- Hardisty, D. S., Lyons, T. W., Riedinger, N., Isson, T. T., Owens, J. D., Aller, R. C., et al. (2018). An evaluation of sedimentary molybdenum and iron as proxies for pore fluid paleoredox conditions. *Am. J. Sci.* 318, 527–556. doi: 10.2475/05.2018.04
- Helz, G. R., Bura-Nakić, E., Mikac, N., and Ciglenečki, I. (2011). New model for molybdenum behavior in euxinic waters. *Chem. Geol.* 284, 323–332. doi: 10.1016/j.chemgeo.2011.03.012
- Helz, G. R., Miller, C. V., Charnock, J. M., Mosselmans, F. W., Patrick, R., Garner, D., et al. (1996). Mechanism of molybdenum removal from the sea and its concentration in black shales: EXAFS evidence. *Geochim. Cosmochim. Acta* 60, 3631–3642. doi: 10.1016/0016-7037(96)00195-0
- Hendy, I. L., and Kennett, J. P. (2000). Dansgaard-Oeschger cycles and the California current system: Planktonic foraminiferal response to rapid climate change in Santa Barbara Basin. Ocean Drilling Program Hole 893A. *Paleoceanogr. Paleoclimatol.* 15, 30–42. doi: 10.1029/1999PA000413
- Hendy, I. L., and Pedersen, T. F. (2006). Oxygen minimum zone expansion in the eastern tropical North Pacific during deglaciation. *Geophys. Res. Lett.* 33:L20602. doi: 10.1029/2006GL025975
- Ho, P., Lee, J.-M., Heller, M. I., Lam, P. J., and Shiller, A. M. (2018). The distribution of dissolved and particulate Mo and V along the U.S. GEOTRACES East Pacific Zonal Transect (GP16): the roles of oxides and biogenic particles in their distributions in the oxygen deficient zone and the hydrothermal plume. *Mar. Chem.* 201, 242–255. doi: 10.1016/j.marchem.2017.12.003
- Hofmann, A. F., Peltzer, E. T., Walz, P. M., and Brewer, P. G. (2011). Hypoxia by degrees: establishing definitions for a changing ocean. *Deep Sea Res. Part I Oceanogr. Res. Pap.* 58, 1212–1226. doi: 10.1016/j.dsr.2011.09.004
- Holmden, C., Amini, M., and Francois, R. (2015). Uranium isotope fractionation in Saanich Inlet: a modern analog study of a paleoredox tracer. *Geochim. Cosmochim. Acta* 153, 202–215. doi: 10.1016/j.gca.2014.11.012
- Hoogakker, B. A. A., Lu, Z., Umling, N., Jones, L., Zhou, X., Rickaby, R. E. M., et al. (2018). Glacial expansion of oxygen-depleted seawater in the eastern tropical Pacific. *Nature* 562, 410–413. doi: 10.1038/s41586-018-0589-x
- Howes, E. L., Joos, F., Eakin, C. M., and Gattuso, J.-P. (2015). An updated synthesis of the observed and projected impacts of climate change on the chemical, physical and biological processes in the oceans. *Front. Mar. Sci.* 2:36. doi: 10.3389/fmars.2015.00036
- Huang, S., and Conte, M. H. (2009). Source/process apportionment of major and trace elements in sinking particles in the Sargasso sea. *Geochim. Cosmochim. Acta* 73, 65–90. doi: 10.1016/j.gca.2008.08.023
- IPCC (2014). Climate Change 2014: Synthesis Report. *Contribution of Working Groups I, II and III to the Fifth Assessment Report of the Intergovernmental Panel on Climate Change [Core Writing Team, R.K. Pachauri and L.A. Meyer (eds.)]. IPCC, Geneva, Switzerland, 151pp.*
- Ivanochko, T. S., Calvert, S. E., Southon, J. R., Enkin, R. J., Baker, J., Dallimore, A., et al. (2008). Determining the post-glacial evolution of a northeast Pacific coastal fjord using a multiproxy geochemical approach. *Can. J. Earth Sci.* 45, 1331–1344. doi: 10.1139/E08-030
- Ivanochko, T. S., and Pedersen, T. F. (2004). Determining the influences of Late Quaternary ventilation and productivity variations on Santa Barbara Basin sedimentary oxygenation: a multi-proxy approach. *Quat. Sci. Rev.* 23, 467–480. doi: 10.1016/j.quascirev.2003.06.006
- Keeling, R. E., Kortzinger, A., and Gruber, N. (2010). Ocean deoxygenation in a warming world. *Ann. Rev. Mar. Sci.* 2, 199–229. doi: 10.1146/annurev.marine.010908.163855
- Klinkhammer, G. P., and Palmer, M. R. (1991). Uranium in the oceans: where it goes and why. *Geochim. Cosmochim. Acta* 55, 1799–1806. doi: 10.1016/0016-7037(91)90024-Y
- Ku, T.-L., Knauss, K. G., and Mathieu, G. G. (1977). Uranium in open ocean: concentration and isotopic composition. *Deep Sea Res.* 24, 1005–1017. doi: 10.1016/0146-6291(77)90571-9
- Lavin, M. F., Castro, R., Beier, E., and Godínez, V. M. (2013). Mesoscale eddies in the southern Gulf of California during summer: characteristics and interaction with the wind stress. *J. Geophys. Res. Oceans* 118, 1367–1381. doi: 10.1002/jgrc.20132
- Lehto, N., Glud, R. N., Á., Norð\*i, G., Zhang, H., and Davison, W. (2014). Anoxic microniches in marine sediments induced by aggregate settlement: biogeochemical dynamics and implications. *Biogeochemistry* 119, 307–327. doi: 10.1007/s10533-014-9967-0
- Levin, L. A. (2018). Manifestation, drivers, and emergence of open ocean deoxygenation. *Ann. Rev. Mar. Sci.* 10, 229–260. doi: 10.1146/annurev-marine-121916-063359
- Long, M. C., Deutsch, C., and Ito, T. (2016). Finding forced trends in oceanic oxygen. *Global Biogeochem. Cycles* 30, 381–397. doi: 10.1002/2015GB005310
- Lovley, D. R., Phillips, E. J. P., Gorby, Y. A., and Landa, E. R. (1991). Microbial reduction of uranium. *Nature* 350, 413–416. doi: 10.1038/350413a0
- Lu, Z., Hoogakker, B. A. A., Hillenbrand, C.-D., Zhou, X., Thomas, E., et al. (2016). Oxygen depletion recorded in upper waters of the glacial Southern Ocean. *Nat. Commun.* 7:11146. doi: 10.1038/ncomms11146

- Lynn, R. J., and Simpson, J. J. (1987). The California Current system: the seasonal variability of its physical characteristics. *J. Geophys. Res. Atmos.* 92, 12947–12966. doi: 10.1029/JC092iC12p12947
- Lyons, T. W., and Berner, R. A. (1992). Carbon-sulfur-iron systematics of the uppermost deep-water sediments of the Black Sea. *Chem. Geol.* 99, 1–27. doi: 10.1016/0009-2541(92)90028-4
- Lyons, T. W., Reinhard, C. T., and Scott, C. (2009). Redox redux. *Geobiology* 7, 489–494. doi: 10.1111/j.1472-4669.2009.00222.x
- Lyons, T. W., and Severmann, S. (2006). A critical look at iron paleoredox proxies: new insights from modern euxinic marine basins. *Geochim. Cosmochim. Acta* 70, 5698–5722. doi: 10.1016/j.gca.2006.08.021
- Mantua, N. J., and Hare, S. R. (2002). The Pacific decadal oscillation. *J. Oceanogr.* 58, 35–44. doi: 10.1023/A:1015820616384
- McKay, J. L., and Pedersen, T. F. (2014). Geochemical response to pulsed sedimentation: implications for the use of Mo as a paleo-proxy. *Chem. Geol.* 382, 83–94. doi: 10.1016/j.chemgeo.2014.05.009
- McManus, J., Berelson, W. M., Coale, K. H., Johnson, K. S., and Kilgore, T. E. (1997). Phosphorus regeneration in continental margin sediments. *Geochim. Cosmochim. Acta* 61, 2891–2907. doi: 10.1016/S0016-7037(97)00138-5
- McManus, J., Berelson, W. M., Klinkhammer, G. P., Johnson, K. S., Coale, K. H., Anderson, R. F., et al. (1998). Geochemistry of barium in marine sediments: implications for its use as a paleoproxy. *Geochim. Cosmochim. Acta* 62, 3453–3473. doi: 10.1016/S0016-7037(98)00248-8
- McManus, J., Berelson, W. M., Severmann, S., Poulson, R. L., Hammond, D. E., Klinkhammer, G. P., et al. (2006). Molybdenum and uranium geochemistry in continental margin sediments: paleoproxy potential. *Geochim. Cosmochim. Acta* 70, 4643–4662. doi: 10.1016/j.gca.2006.06.1564
- McPhaden, M. J. (2004). Evolution of the 2002/03 El Niño\*. *Bull. Am. Meteorol. Soc.* 85, 677–695. doi: 10.1175/BAMS-85-5-677
- Metcalfe, S. E., Barron, J. A., and Davies, S. J. (2015). The Holocene history of the North American Monsoon: 'known knowns' and 'known unknowns' in understanding its spatial and temporal complexity. *Quat. Sci. Rev.* 120, 1–27. doi: 10.1016/j.quascirev.2015.04.004
- Moffitt, S. E., Moffitt, R. A., Sauthoff, W., Davis, C. W., Hewett, K., and Hill, T. M. (2015). Paleoceanographic insights on recent oxygen minimum zone expansion: lessons for modern oceanography. *PLoS ONE* 10: e0115246. doi: 10.1371/journal.pone.0115246
- Monreal-Gómez, M. A., Molina-Cruz, A., and Salas-de-León, D. A. (2001). Water masses and cyclonic circulation in Bay of la Paz, Gulf of California, during June 1998. *J. Mar. Syst.* 30, 305–315. doi: 10.1016/S0924-7963(01)00064-1
- Morford, J. L., and Emerson, S. (1999). The geochemistry of redox sensitive trace metals in sediments. *Geochim. Cosmochim. Acta* 63, 1735–1750. doi: 10.1016/S0016-7037(99)00126-X
- Morse, J. W., and Luther, G. W. III. (1999). Chemical influences on trace metal-sulfide interactions in anoxic sediments. *Geochim. Cosmochim. Acta* 63, 3373–3378. doi: 10.1016/S0016-7037(99)00258-6
- Moy, C. M., Seltzer, G. O., Rodbell, D. T., and Anderson, D. M. (2002). Variability of El Niño/Southern Oscillation activity at millennial timescales during the Holocene epoch. *Nature* 420, 162–165. doi: 10.1038/nature01194
- Nameroff, T. J., Calvert, S. E., and Murray, J. W. (2004). Glacial-interglacial variability in the eastern tropical North Pacific oxygen minimum zone recorded by redox-sensitive trace metals. *Paleoceanogr. Paleoclimatol.* 19:PA1010. doi: 10.1029/2003PA000912
- Nava-Sánchez, E. H., Gorsline, D. S., and Molina-Cruz, A. (2001). The Baja California peninsula borderland: structural and sedimentological characteristics. *Sediment. Geol.* 144, 63–82. doi: 10.1016/S0037-0738(01)00135-X
- Ontiveros-Cuadras, J. F., Thunell, R., Ruiz-Fernández, A. C., Benitez-Nelson, C., Machain-Castillo, M. L., Tappa, E., et al. (2019). Centennial OMZ changes in the NW Mexican Margin from geochemical and foraminiferal sedimentary records. *Cont. Shelf Res.* 176, 64–75. doi: 10.1016/j.csr.2019.02.009
- Oschlies, A., Schulz, K. G., Riebesell, U., Schmittner, A. (2008). Simulated 21st century's increase in oceanic suboxia by CO<sub>2</sub>-enhanced biotic carbon export. *Global Biogeochem. Cycles* 22:GB4008. doi: 10.1029/2007GB003147
- Pérez-Cruz, L. (2013). Hydrological changes and paleoproductivity in the Gulf of California during middle and late Holocene and their relationship with ITCZ and North American Monsoon variability. *Quat. Res.* 79, 138–151. doi: 10.1016/j.yqres.2012.11.007
- Pichevin, L., Ganeshram, R. S., Reynolds, B. C., Prahl, F., Pedersen, T. F., Thunell, R., et al. (2012). Silicic acid biogeochemistry in the Gulf of California: Insights from sedimentary Si isotopes. *Paleoceanogr. Paleoclimatol.* 27:PA2201. doi: 10.1029/2011PA002237
- Pichevin, L. E., Ganeshram, R. S., Geibert, W., Thunell, R., and Hinton, R. (2014). Silica burial enhanced by iron limitation in oceanic upwelling margins. *Nat. Geosci.* 7, 541–546. doi: 10.1038/ngeo2181
- Praetorius, S. K., Mix, A. C., Walczak, M. H., Wolhowe, M. D., Addison, J. A., and Prahl, F. G. (2015). North Pacific deglacial hypoxic events linked to abrupt ocean warming. *Nature* 527, 362–366. doi: 10.1038/nature15753
- Raiswell, R., and Canfield, D. E. (2012). The iron biogeochemical cycle past and present. *Geochem. Perspect.* 1, 1–220. doi: 10.7185/geochempersp.1.1
- Reck, B. K., Müller, D. B., Rostkowski, K., and Graedel, T. E. (2008). Anthropogenic nickel cycle: insights into use, trade, and recycling. *Environ. Sci. Technol.* 42, 3394–3400. doi: 10.1021/es072108l
- Reimer, P. J., Bard, E., Bayliss, A., Beck, J. W., Blackwell, P. G., Ramsey, C. B., et al. (2013). IntCal13 and Marine13 Radiocarbon Age Calibration Curves 0–50,000 Years cal BP. *Radiocarbon* 55, 1869–1887. doi: 10.2458/azu\_rc.55.16947
- Riedinger, N., Brunner, B., Krastel, S., Arnold, G. L., Wehrmann, L. M., Formolo, M. J., et al. (2017). Sulfur cycling in an iron oxide-dominated, dynamic marine depositional system: the Argentine continental margin. *Front. Earth Sci.* 5:33. doi: 10.3389/feart.2017.00033
- Riedinger, N., Formolo, M. J., Lyons, T. W., Henkel, S., Beck, A., and Kasten, S. (2014). An inorganic geochemical argument for coupled anaerobic oxidation of methane and iron reduction in marine sediments. *Geobiology* 12, 172–181. doi: 10.1111/gbi.12077
- Riedinger, N., Kasten, S., Gröger, J., Franke, C., and Pfeifer, K. (2006). Active and buried authigenic barite fronts in sediments from the Eastern Cape Basin. *Earth Planet. Sci. Lett.* 241, 876–887. doi: 10.1016/j.epsl.2005.10.032
- Rodríguez-Castañeda, A. P. (2008). Variación de flujos de los elementos particulados en Cuenca Alfonso, Bahía de La Paz, en el periodo 2002–2005. [Ph.D. dissertation]. [La Paz, Mexico]: Centro Interdisciplinario de Ciencias Marinas – Instituto Politécnico Nacional
- Ruiz-Fernández, A. C., Hillaire-Marcel, C., De Vernal, A., Machain-Castillo, M. L., Vásquez, L., Ghaleb, B., et al. (2009). Changes of coastal sedimentation in the Gulf of Tehuantepec, South Pacific Mexico, over the last 100 years from short-lived radionuclide measurements. *Estuar. Coast. Shelf Sci.* 82, 525–536. doi: 10.1016/j.ecss.2009.02.019
- Schmidtko, S., Stramma, L., and Visbeck, M. (2017). Decline in global oceanic oxygen content during the past five decades. *Nature* 542, 335–339. doi: 10.1038/nature21399
- Schneider, T., Bischoff, T., and Haug, G. H. (2014). Migrations and dynamics of the intertropical convergence zone. *Nature* 513, 45–53. doi: 10.1038/nature13636
- Schoepfer, S. D., Shen, J., Wei, H., Tyson, R. V., Ingall, E., and Algeo, T. J. (2015). Total organic carbon, organic phosphorus, and biogenic barium fluxes as proxies for paleomarine productivity. *Earth Sci. Rev.* 149, 23–52. doi: 10.1016/j.earscirev.2014.08.017
- Scholz, F. (2018). Identifying oxygen minimum zone-type biogeochemical cycling in Earth history using inorganic geochemical proxies. *Earth Sci. Rev.* 184, 29–45. doi: 10.1016/j.earscirev.2018.08.002
- Scholz, F., Hensen, C., Noffke, A., Rohde, A., Liebetrau, V., and Wallmann, K. (2011). Early diagenesis of redox-sensitive trace metals in the Peru upwelling area – response to ENSO-related oxygen fluctuations in the water column. *Geochim. Cosmochim. Acta* 75, 7257–7276. doi: 10.1016/j.gca.2011.08.007
- Scholz, F., Siebert, C., Dale, A. W., and Frank, M. (2017). Intense molybdenum accumulation in sediments underneath a nitrogenous water column and implications for the reconstruction of paleo-redox conditions based on molybdenum isotopes. *Geochim. Cosmochim. Acta* 213, 400–417. doi: 10.1016/j.gca.2017.06.048
- Scott, C., and Lyons, T. W. (2012). Contrasting molybdenum cycling and isotopic properties in euxinic versus non-euxinic sediments and sedimentary rocks: refining the paleoproxies. *Chem. Geol.* 324–325, 19–27. doi: 10.1016/j.chemgeo.2012.05.012
- Shaffer, G., Olsen, S. M., and Pedersen, J. O. P. (2009). Long-term ocean oxygen depletion in response to carbon dioxide emissions from fossil fuels. *Nat. Geosci.* 2, 105–109. doi: 10.1038/ngeo420
- Silverberg, N., Aguirre-Bahena, F., and Mucci, A. (2014). Time-series measurements of settling particulate matter in Alfonso Basin, La Paz

- Bay, southwestern Gulf of California. *Cont. Shelf Res.* 84, 169–187. doi: 10.1016/j.csr.2014.05.005
- Staines-Urias, F., González-Yajimovich, O., and Beaufort, L. (2015). Reconstruction of past climate variability and ENSO-like fluctuations in the southern Gulf of California (Alfonso Basin) since the last glacial maximum. *Q. Res.* 83, 488–501. doi: 10.1016/j.yqres.2015.03.007
- Tems, C. E., Berelson, W. M., and Prokopenko, M. G. (2015). Particulate  $\delta^{15}\text{N}$  in laminated marine sediments as a proxy for mixing between the California Undercurrent and the California Current: a proof of concept. *Geophys. Res. Lett.* 42, 419–427. doi: 10.1002/2014GL061993
- Tems, C. E., Berelson, W. M., Thunell, R., Tappa, E., Xu, X., Khider, D., et al. (2016). Decadal to centennial fluctuations in the intensity of the eastern tropical North Pacific oxygen minimum zone during the last 1200 years. *Paleoceanography Paleoclimatol.* 31, 1138–1151. doi: 10.1002/2015PA002904
- Tetard, M., Licari, L., and Beaufort, L. (2017). Oxygen history off Baja California over the last 80 kyr: a new foraminiferal-based record. *Paleoceanography Paleoclimatol.* doi: 10.1002/2016PA003034
- Thunell, R. (1998). Seasonal and annual variability in particle fluxes in the Gulf of California. *A response to climate forcing. Deep Sea Res. Part I Oceanogr. Res. Pap.* 45, 2059–2083. doi: 10.1016/S0967-0637(98)00053-3
- Trasviña-Castro, A., Gutierrez De Velasco, G., Valle-Levinson, A., González-Armas, R., Muhlia, A., and Cosío, M. A. (2003). Hydrographic observations of the flow in the vicinity of a shallow seamount top in the Gulf of California. *Estuar. Coast. Shelf Sci.* 57, 149–162. doi: 10.1016/S0272-7714(02)00338-4
- Tribovillard, N., Algeo, T. J., Lyons, T., and Riboulleau, A. (2006). Trace metals as paleoredox and paleoproductivity proxies: an update. *Chem. Geol.* 232, 12–32. doi: 10.1016/j.chemgeo.2006.02.012
- Tribovillard, N., Bout-Roumazeilles, V., Algeo, T., Lyons, T. W., Sionneau, T., Montero-Serrano, J. C., et al. (2008). Paleodepositional conditions in the Orca Basin as inferred from organic matter and trace metal contents. *Mar. Geol.* 254, 62–72. doi: 10.1016/j.margeo.2008.04.016
- Twining, B. S., Baines, S. B., Vogt, S., and Nelson, D. M. (2012). Role of diatoms in nickel biogeochemistry in the ocean. *Glob. Biogeochem. Cycles* 26. doi: 10.1029/2011GB004233
- Umling, N. E., and Thunell, R. C. (2017). Synchronous deglacial thermocline and deep-water ventilation in the eastern equatorial Pacific. *Nat. Commun.* 8:14203. doi: 10.1038/ncomms14203
- Wedepohl, K. H. (1995). The composition of the continental crust. *Geochim. Cosmochim. Acta* 59, 1217–1232. doi: 10.1016/0016-7037(95)00038-2
- Wignall, P. B., and Myers, K. J. (1988). Interpreting benthic oxygen levels in mudrocks: a new approach. *Geology* 16:452–455. doi: 10.1130/0091-7613(1988)016<0452:IBOLIM>2.3.CO;2
- World Ocean Atlas (2005). [http://www.nodc.noaa.gov/OC5/WOA05/pr\\_woa05.html](http://www.nodc.noaa.gov/OC5/WOA05/pr_woa05.html)
- Wright, J. J., Konwar, K. M., and Hallam, S. J. (2012). Microbial ecology of expanding oxygen minimum zones. *Nat. Rev. Microbiol.* 10, 381–394. doi: 10.1038/nrmicro2778
- Yan, H., Sun, L., Wang, Y., Huang, W., Qiu, S., and Yang, C. (2011). A record of the Southern Oscillation Index for the past 2,000 years from precipitation proxies. *Nat. Geosci.* 4, 611–614. doi: 10.1038/ngeo1231
- Zheng, Y., Anderson, R. B., Van Geen, A., and Fleisher, M. Q. (2002). Preservation of particulate non-lithogenic uranium in marine sediments. *Geochim. Cosmochim. Acta* 66, 3085–3092. doi: 10.1016/S0016-7037(01)00632-9
- Zheng, Y., Anderson, R. B., Van Geen, A., and Kuwabara, J. (2000). Authigenic molybdenum formation in marine sediments: a link to pore water sulfide in Santa Barbara Basin. *Geochim. Cosmochim. Acta* 64, 4165–4178. doi: 10.1016/S0016-7037(00)00495-6

**Conflict of Interest Statement:** The authors declare that the research was conducted in the absence of any commercial or financial relationships that could be construed as a potential conflict of interest.

Copyright © 2019 Choumiline, Pérez-Cruz, Gray, Bates and Lyons. This is an open-access article distributed under the terms of the Creative Commons Attribution License (CC BY). The use, distribution or reproduction in other forums is permitted, provided the original author(s) and the copyright owner(s) are credited and that the original publication in this journal is cited, in accordance with accepted academic practice. No use, distribution or reproduction is permitted which does not comply with these terms.